Published in final edited form as:

Pain. 2015 September ; 156(9): 1620–1636. doi:10.1097/j.pain.0000000000000224.

Induction of Thermal and Mechanical Hypersensitivity by Parathyroid Hormone-related Peptide (PTHrP) Through Upregulation of TRPV1 Function and Trafficking

Aaron D. Mickle[a,b], **Andrew J. Shepherd**[a,b], **Lipin Loo**[a,#], and **Durga P. Mohapatra**[a,b,c,*]

[a]Department of Pharmacology, The University of Iowa Roy J. and Lucile A. Carver College of Medicine, Iowa City, IA, USA

[b]Department of Anesthesiology, and Washington University Pain Center, Washington University School of Medicine, St. Louis, MO, USA

[c]Department of Anesthesia, The University of Iowa Roy J. and Lucile A. Carver College of Medicine, Iowa City, IA, USA

Abstract

The neurobiological mechanisms underlying chronic pain associated with cancers are not well understood. It has been hypothesized that factors specifically elevated in the tumor microenvironment sensitize adjacent nociceptive afferents. We show that parathyroid hormone-related peptide (PTHrP), which is found at elevated levels in the tumor microenvironment of advanced breast and prostate cancers, is a critical modulator of sensory neurons. Intraplantar injection of PTHrP led to the development of thermal and mechanical hypersensitivity in both male and female mice, which were absent in mice lacking functional transient receptor potential vanilloid-1 (TRPV1). The PTHrP treatment of cultured mouse sensory neurons enhanced action potential firing, and increased TRPV1 activation, which was dependent on protein kinase C (PKC) activity. Parathyroid hormone-related peptide induced robust potentiation of TRPV1 activation and enhancement of neuronal firing at mild acidic pH that is relevant to acidic tumor microenvironment. We also observed an increase in plasma membrane TRPV1 protein levels after exposure to PTHrP, leading to upregulation in the proportion of TRPV1-responsive neurons, which was dependent on the activity of PKC and Src kinases. Furthermore, co-injection of PKC or Src inhibitors attenuated PTHrP-induced thermal but not mechanical hypersensitivity. Altogether, our results suggest that PTHrP and mild acidic conditions could induce constitutive pathological activation of sensory neurons through upregulation of TRPV1 function and trafficking, which could serve as a mechanism for peripheral sensitization of nociceptive afferents in the tumor microenvironment.

[*]Author to whom all correspondence should be addressed at: D.P. Mohapatra, Ph.D., Department of Anesthesiology, and Washington University Pain Center, Washington University School of Medicine, 5502 CSRB, 660 S. Euclid Avenue, St. Louis, MO, 631010; Tel. (314) 362 8229; mohapatrad@anest.wustl.edu.

[#]Present address: Department of Cell Biology and Physiology, UNC Neuroscience Center, University of North Carolina, Chapel Hill, NC.

Conflict of Interest Statement:

The authors have no conflicts of interest to declare

1. INTRODUCTION

Despite many advances in cancer research, treatment for the associated pain conditions has gone mostly overlooked and under-managed [62,68]. Chronic pain in cancers, such as breast and prostate, are primarily treated with opioids, which over prolonged treatment durations lead to decreased efficacy, increased tolerance, and even promotion of tumor growth [20,51]. Moreover, the precise neurobiological mechanisms underlying this pain remain unknown, which poses a serious challenge for the development of efficacious analgesics. Specific factors secreted into the tumor microenvironment have been proposed to sensitize adjacent nociceptive fibers, thereby causing chronic pain [20,48,50,51,81]. Parathyroid hormone-related peptide (PTHrP), which is expressed at high levels in advanced breast and prostate tumors, could represent one of these factors. Knock-down and/or antibody-neutralization of PTHrP have been shown to dramatically reduce the frequency of metastasis and subsequent tumor growth [17,30,43,45,46,66,89]. PTHrP activates parathyroid hormone receptor 1 (PTH1R), which is a $G\alpha_q$- or $G\alpha_s$- protein-coupled receptor [1], resulting in downstream activation of protein kinases C (PKC) and/or A (PKA), both of which are critical to its tumor-promoting effects [31,41,78].

It is well established that activation of PKC and PKA enhance sensory neuron firing via modulation of the transient receptor potential vanilloid-1 (TRPV1) [15,22,38,44,70,71]. TRPV1 is a polymodal detector of noxious stimuli, mainly noxious temperatures (>43°C), acidic pH (<pH 6.0), and several endogenous and exogenous compounds [11,38]. Post-translational modification of TRPV1 by PKC, PKA, microtubule-associated protein kinases, and Src kinases dramatically potentiate channel function and expression [6,7,35,37,57,63,70,87,90], leading to channel activation at or below body temperatures (<37°C) and/or to mild acidic pH ranges [15,47,63,70]. Involvement of TRPV1 in cancer pain has been reported in rodent models of bone sarcoma and cutaneous cancers [4,15,21,48,50,51,65,76,79]. Tumor-related factors such as granulocyte colony-stimulating factor (G-CSF), granulocyte-macrophage colony stimulating-factor (GM-CSF), interleukin-6 (IL-6), tumor necrosis factor-alpha (TNF-α), nerve growth factor, (NGF), and lysophosphatidic acid (LPA) have previously been shown to modulate the activity of TRPV1, and are therefore considered as mediators of tumor-nerve interactions [3,15,24,44,48,50,65,76,81].

We hypothesized that PTHrP could potentiate sensory neuron excitation via upregulating TRPV1 channel function, thereby providing a mechanism for peripheral pain sensitization. We demonstrate that PTHrP induced peripheral thermal and mechanical hypersensitivity in mice, which were absent in TRPV1 knock-out (*Trpv1*$^{-/-}$) mice. PTHrP increased sensory neuron excitability via PKC-dependent enhancement of TRPV1 currents. Additionally, PTHrP caused a Src-dependent increase in plasma membrane TRPV1 levels, resulting in increased proportion of functional TRPV1-expressing neurons. Interestingly, Src inhibition attenuated PTHrP-induced thermal hypersensitivity in mice, suggesting a critical role for increased TRPV1 trafficking in peripheral nociceptor sensitization by PTHrP. This could presumably sub-serve a mechanism for peripheral pain sensitization associated with breast/prostate cancers.

2. MATERIALS AND METHODS

All experiments were performed using adult (6–14 weeks old) mice housed in The University of Iowa animal facility on a 12-hour light/dark cycle with access to food and water *ad libitum*. All the procedures involving mice and mouse tissue performed in this study were approved by the University of Iowa Institutional Animal Care and Use Committee, and in strict accordance the US *National Institute of Health (NIH) Guide for the Care and Use of Laboratory Animals*. Every effort was made to minimize the number of mice used in this study and their suffering. All female mice used in this study were not staged to ascertain any specific part of their estrous cycle, and all the behavioral and DRG isolation experiments on female mice were performed irrespective of any specific sage of their estrous cycle.

2.1. Chemicals and reagents

Purified recombinant human/rodent collagenase and pronase were purchased from EMD-Millipore Chemicals, Billerica, MA, and the Ca^{2+}-sensitive dye Fura-2AM and pluronic acid were purchased from Life Technologies, Grand Island, NY. PTHrP was from Peprotech, Rockhill, NJ; capsaicin was from Sigma-Aldrich, St. Louis, MO; PKC activator phorbol 12-myristate 13-acetate (PMA), PKC inhibitor bisindoylmelimide-I (BIM-I), PKA activator forskolin [[3*R*-(3α,4aβ,5β,6β,6aα,10α,10aβ,10bα)]-5-(Acetyloxy)-3-ethenyldodecahydro-6,10,10b-trihydroxy-3,4a,7,7,10a-pentamethyl-1*H*-naphtho[2,1-*b*]pyran-1-one], PKA inhibitor KT5720 [(9*S*,10*R*,12*R*)-2,3,9,10,11,12-hexahydro-10-hydroxy-9-methyl-1-oxo-9,12-epoxy-1 *H*-diindolo[1,2,3-fg:3′,2′,1′-kl]pyrrolo[3,4-i][1,6]benzodiazocine-10-carboxylicacid hexyl ester], and the Src kinase inhibitor PP2 [3-(4-chlorophenyl) 1-(1,1-dimethylethyl)-1*H*-pyrazolo[3,4-*d*]pyrimidin-4-amine] were from Tocris Bioscience-Bio-Techne, Minneapolis, MN. Cyclic adenosine monophosphate (cAMP) enzyme-linked immunosorbent assay (ELISA) kits were purchased from Enzo Life Sciences, Farmingdale, NY, and the cellular membrane fractionation kit was purchased from Invent Biotechnologies, Eden Prairie, MN. All other chemicals and reagents in this study were purchased from Sigma-Aldrich, St. Louis, MO, Bio-Rad, Roche Applied Science, Indianapolis, IN, Life Technologies, Grand Island, NY, and Thermo Fisher Scientific, Waltham, MA.

2.2. Behavioral assessment of thermal and mechanical hypersensitivity

Adult C57BL/6 mice of *Trpv1*$^{+/+}$ (wild-type) and *Trpv1*$^{-/-}$ genotype were acclimated to the testing environments of thermal and mechanical hypersensitivities for 2 days prior to testing by placing them in the testing chambers for 30 min two times a day separated by at least 1 hour. Thermal hypersensitivity was tested as described previously [47] using a plantar test apparatus (IITC Life Sciences, Woodland Hills, CA). Briefly, mice were placed in individual Plexiglas testing chambers situated on a glass plate maintained at thermo-neutral temperature (~30°C) for 30 min before testing. Tests were conducted by applying a focused high-intensity beam of light on the plantar surface of the hind paw and the duration or latency to paw withdrawal was recorded using a programmable digital counter. For each time point, the paw withdrawal latency (PWL) was measured for both limbs twice and the average was taken for analysis.

Mechanical sensitivity was measured using a range of 8 Von Frey hair filaments (0.04 – 2 g; Stoelting Co., Wood Dale, IL) applied to the plantar surface of the mouse hind paw. Mice were placed on a wire mesh platform covered by a Plexiglas box for 15 min before testing. Tests were performed starting with the lowest filament strength (0.04 g) and moving up to the filament with maximum strength (2 g), each filament was applied to individual mouse hind paw five times, and the number of paw withdrawal responses was recorded as percentage of response. To access the changes in paw withdrawal response to the whole range of filaments over testing durations, the area under the curve (AUC) was calculated for each animal and the average AUC for each treatment group was calculated, similar to the analysis method described earlier [5] with some modifications.

Baseline measurements were taken for both thermal and mechanical sensitivity, and then followed by intraplantar (i.pl.) injection of saline or different concentrations of PTHrP (10 μl of 20 nM, 100 nM, 200 nM, 1 μM or 20 μM) into one hind paw with a 33-gauge needle coupled to a microsyringe. Thermal sensitivity was measured at 0.5, 5.5 and 24 hours after injections, and mechanical sensitivity was measured at 1, 6 and 24 hours after injections. In separate experimental groups BIM-I (10 μg) or PP2 (3 μg) were co-injected along with PTHrP or alone. Saline-injected and PTHrP-injected controls were included in every cohort of animals tested. The experimenter performing behavioral assessment of thermal and mechanical hypersensitivity was blinded to the lateralization and details of drug injections, as well as to the genotypes of mice. All behavioral experiments were performed on 6 to 12 mice of individual genotypes (wherever mentioned), in 2 or more cohorts of animals.

2.3. Primary cultures of mouse DRG neurons

DRGs were isolated from adult *Trpv1*$^{+/+}$ and *Trpv1*$^{-/-}$ mice of both sexes in the C57BL/6 background, following the procedure described previously [15,47]. Isolated DRGs were dissociated and digested with the enzymes collagenase and pronase, and then plated onto poly-L-ornithine- and laminin-coated glass coverslips (for Ca^{2+} imaging) or 14 mm glass bottom dishes (Mat-Tek Co., Ashland, MA; for biochemical experiments). Cells were incubated in culture media comprised a of 1:1 ratio of TNB media supplemented with protein-lipid complex (Biochrom AG, Germany) and Dulbecco's modified-Eagle's medium (DMEM) supplemented with 10% fetal bovine serum at 37°C in a 5% CO_2 incubator for 2–3 days, before using in Ca^{2+} imaging, biochemical and electrophysiological experiments.

2.4. Electrophysiology and data analysis

All voltage- and current-clamp experiments on cultured mouse DRG neurons were performed as per the protocols described previously [47]. For voltage-clamp experiments the pipette solution contained (in mM): 5 NaCl, 140 KCl, 1 $CaCl_2$, 1 $MgCl_2$, 10 HEPES, 5 EGTA and 3 Na-ATP, pH 7.3 with KOH. The cells were bathed in extracellular buffer containing (in mM) 140 NaCl, 5 KCl, 0.1 $CaCl_2$, 1 $MgCl_2$, 10 HEPES, 10 glucose, and 1 tetrodotoxin, pH 7.3 with NaOH. Low extracellular Ca^{2+} concentration was used to minimize the Ca^{2+}-dependent desensitization of TRPV1 [59]. For proton dose-response experiments, Ca^{2+}-free extracellular buffers were used, in order to inhibit TRPV1 channel desensitization, and HEPES was substituted with 2-(N-Morpholino)ethanesulfonic acid sodium salt in extracellular buffers with pH 5.8, 5.4, and 4.8. All drugs were diluted in

extracellular buffer and perfused locally onto the cell under recording, using individual channels of a Teflon tubing-connected glass multiple-barrel gravity driven perfusion system. Currents were recorded at room temperature (~22°C) with an Axopatch 200B patch-clamp amplifier connected to a Digidata 1440A data acquisition system (Molecular Devices, Sunnyvale, CA). The holding potential was −70 mV, and the data were sampled at 2 kHz and filtered at 1 kHz using pClamp 10 software (Molecular Devices, Sunnyvale, CA). Patch pipettes were pulled from borosilicate glass tubes and heat polished at the tip using a microforge (World Precision Instruments, Sarasota, FL) to give a resistance of 2–6 MΩ when filled with the pipette solution. Clampfit 10 (Molecular Devices, Sunnyvale, CA), Excel (Microsoft Co, Redmond, WA), and Prism 6 (GraphPad Software, San Diego, CA) software were used for the analysis of currents and preparing traces/figures. Data are presented as means ± SEM or fitted value ± SE of the PTHrP and pH dose-response curve Hill equation fits.

For current-clamp experiments the extracellular solution contained (in mM): 140 NaCl, 5 KCl, 2 $CaCl_2$, 1 $MgCl_2$, 10 HEPES and 10 glucose, pH 7.3 with NaOH. The pipette solution was the same as in voltage-clamp experiments. Action potentials (AP) were evoked by perfusing capsaicin-containing or acidic-pH extracellular buffer directly onto the cell under current-clamp mode. The number of APs were counted during the first 5 sec of perfusion and normalized to 5 sec before agonist application to determine the evoked firing frequency. Spontaneous APs were calculated as the number of APs per sec during PTHrP or extracellular buffer (control) applications. All electrophysiology experiments were performed on five or more batches of mouse DRG neuron cultures.

2.5. Reverse transcription polymerase chain reaction

Total RNA was isolated from female C57BL/6 mouse DRGs using TRIzol reagent (Invitrogen), treated with DNase-I for 30 min at 37°C, and followed by 65°C to inactivate the enzyme. The RNA was then reverse-transcribed into cDNA using a SuperScript III RT-PCR kit (Invitrogen). Individual PCR reactions were then performed using the cDNA Choice Blue Master Mix (Denvile Scientific Inc), and specific primers targeting mouse PTH1R (forward 5′-GCAGTACCTTGTCCCGATTA-3′; and reverse 5′-CGCAGCATAAACGACAGGA-3′). PCR products were electrophoretically size fractionated in a 0.7% agarose gel and stained with ethidium bromide, to visualize amplified PCR products and to verify their predicted size. Experiments were performed on DRGs isolated from 3 or more mice.

2.6. Immunostaining of DRG sections, cultured neurons, and HEK293T cells

Lumbar DRGs (L4–L6) were harvested from adult female C57BL/6 mice perfused with 4% paraformaldehyde (PFA) for 20 min, as described previously [47,77]. The DRGs were stored in 4% PFA with 5% picric acid overnight and were then transferred into 15% sucrose solution in 0.1 M phosphate buffer (PB) for 24 hours. DRGs were mounted in optimal cutting temperature (OCT) compound (Sakura Finetek USA Inc., Torrance, CA), and 25 μm thick sections were obtained using a cryostat (Leica, Buffalo Grove, IL). Free-floating DRG sections were stained as described previously [47]. Sections were incubated with guinea pig polyclonal antibody against TRPV1 (1:200; Neuromics, Edina, MN) and mouse monoclonal

antibody against PTH1R (1:200; Millipore, Billerica, MA) with blocking solution overnight at 4°C. After washing 3 times for 10 min each, sections were incubated with donkey anti-mouse IgG conjugated with Alexa Fluor-555 and donkey anti-guinea pig IgG conjugated with Alexa Fluor-488 secondary antibodies (both 1:1000; Life Technologies, Grand Island, NY) for 3 hours. After washing three times for 10 min each, sections were transferred to glass slides and mounted with ProlongGold anti-fade agent (Life Technologies, Grand Island, NY). Confocal fluorescence images of mouse DRG sections were taken using a BX61WI microscope equipped with the Fluoview 300 laser-scanning confocal imaging system (Olympus, Waltham, MA) with a 10X objective (NA 0.25; Olympus). All immunohistochemical experiments were performed on DRGs from five or more mice. Cells in mouse DRG sections that are co-labeled for both TRPV1 and PTH1R, as well as for either TRPV1 or PTH1R staining were counted on multiple sections in a blinded fashion, in order to determine the overlap between TRPV1 and PTH1R expression in DRGs.

HEK293T cells transfected (using lipofectamine2000; Invitrogen) with plasmid containing yellow fluorescent protein (YPF)-tagged recombinant mouse PTH1R cDNA (in peYFP-N1 vector) were fixed 42–48 hours post-transfection with 4% PFA. Cells were blocked and stained with mouse monoclonal antibody against PTH1R (1:200; Millipore, Billerica, MA). After washing cells were incubated with goat anti-mouse IgG conjugated with Alexa Fluor-555 (1:2000; Invitrogen) and DAPI nuclear stain (1:5000), and then mounted onto glass slides. Immunofluorescence images of cells were captured using a MRc-5 digital camera connected to a Zeiss AxioImager epifluorescence microscope, using the AxioVision software (Carl Zeiss, Thornwood, NY), with a 63X Plan-Apochromat objective (NA 1.4; Carl Zeiss). All the images were transferred to Photoshop software (Adobe Systems, San Jose, CA) as TIFF files.

PKCε translocation assays on cultured mouse DRG neurons on glass coverslips were performed as described previously [47]. Cells were treated with PTHrP (for 5, 15 and 30 min) or 100 nM PMA (2 min), fixed with 4% PFA, and stained with rabbit polyclonal antibody against PKCε (1:500; BD Bioscience, San Jose, CA) and mouse monoclonal antibody against TRPV1 (5 μg/ml; clone N221/17; NeuroMab, Davis, CA) or mouse monoclonal antibody against PTH1R (1:200; Millipore, Billerica, MA). After washing cells were incubated with goat anti-mouse IgG conjugated with Alexa Fluor-488 and goat anti-rabbit IgG conjugated with Alexa Fluor-555 secondary antibodies (both 1:2000; Life Technologies, Grand Island, NY), and then mounted onto glass slides. Confocal fluorescence images of DRG neurons were taken using a BX61WI microscope equipped with the Fluoview 300 laser-scanning confocal imaging system (Olympus, Waltham, MA) with a 60X objective (NA 1.4; Olympus). Individual images were analyzed using NIH ImageJ software for translocation of PKCε to the cell periphery, as described previously [47]. The experimenter was blinded to the treatment groups, and the results are expressed as percentage of neurons exhibiting cell periphery-enriched (translocated) vs uniformly distributed (non-translocated) PKCε signals. All immunocytochemical experiments on cultured mouse DRG were performed on three or more batches of mouse DRG neuron cultures.

2.7. Functional Ca^{2+} imaging

Ca^{2+} imaging experiments on cultured mouse DRG neurons were performed as described previously [47]. The standard extracellular HEPES-buffered HBSS (HH buffer) contained (in mM) 140 NaCl, 5 KCl, 1.3 $CaCl_2$, 0.4 $MgSO_4$, 0.5 $MgCl_2$, 0.4 KH_2PO_4, 0.6 $NaHPO_4$, 3 $NaHCO_3$, 10 glucose, and 10 HEPES, pH 7.35 with NaOH (310 mOsm/kg with sucrose). Briefly, cultured DRG neurons on glass coverslips were incubated with 1.5 μM of Fura-2AM for 30 min at room temperature (~22°C) prior to the experiment. The coverslip was washed in HH buffer following incubation to remove excess dye and then placed in the recording chamber mounted on the stage of an inverted IX-71 microscope (Olympus, Waltham, MA), followed by another 10 min of wash with HH buffer before the experiment began. Fluorescence was alternately excited at 340 and 380 nm using the Polychrome IV monochromator (T.I.L.L. Photonics, Germany), via a 20X objective [numerical aperture (NA) 0.75; Olympus], and the emitted fluorescence was collected at 510 (80) nm using an IMAGO CCD camera (T.I.L.L. Photonics, Germany). Pairs of 340/380 nm images were sampled at 0.2 Hz. Bath application of two consecutive capsaicin applications (15 s) in HH buffer was performed with a 5 min interval. Only two capsaicin applications were given in these experiments, in order to prevent massive increase in intracellular Ca^{2+} ($[Ca^{2+}]_i$) levels in DRG neurons, which often leads to subsequent TRPV1-independent intracellular Ca^{2+} release/flux. Such high levels of $[Ca^{2+}]_i$ levels induce strong desensitization of TRPV1 [6,7,42,57–59], and thereby occludes the actual magnitude of channel sensitization. The recording chamber was perfused globally with HH buffer or PTHrP or PMA, without or with pharmacological inhibitors of protein kinases during the entire 5 min inter-capsaicin interval duration, in order to provide sufficient time duration for the action of drugs to take place. Relative capsaicin-induced peak Ca^{2+} levels were measured by the ratio of 340 nm to 380 nm excitations. Data were analyzed as a ratio of the 2^{nd} over 1^{st} capsaicin-induced peak Ca^{2+} levels and presented as mean ± SEM, in order to determine the magnitude of TRPV1 channel sensitization. All Ca^{2+} imaging experiments were performed on five or more batches of mouse DRG neuron cultures.

2.8. Transfection of mouse DRG neurons

Mouse DRGs were collected and cells were isolated and digested with collagenase and pronase enzymes as described above. Before plating, cell suspensions were transfected with Nucleofection kit (Lonza, Switzerland) following the primary mouse DRG neuron small cell number (SCN) transfection protocol. Cells were combined with 100 μl of Basic Neuron SCN Nucleofector® solution and 20 μl of SCN Supplement, this mixture was then combined with 1 μg of plasmid containing pmaxGFP® and 2.5 μg plasmid containing the dominant-negative Src (DN-Src) and placed in an SCN cuvette. Cuvette was then placed in an Amaxa Nucleofector™ II using the SCN neuron transfection protocol (G-013). Separate batches of mouse DRG neuron were also prepared with the transfection of 3.5 μg of plasmid containing pmaxGFP®, to serve as transfection control group. Cells were then plated on to poly-L-ornithine- and laminin-coated glass coverslips and the DRG cell culture protocol was followed, as mentioned above.

2.9. Cyclic adenosine monophosphate enzyme-linked immunosorbent assay

Acutely dissociated mouse DRGs were treated with either 20 nM PTHrP (5, 15 and 30 min) or 10 μM forskolin (5 min) and then lysed in 0.1 N HCl by incubating on ice for 20 min and vortexing several times throughout the incubation duration. Total protein levels in lysates were quantified by bicinchoninic acid (BCA) method (Thermo-Pierce Scientific, Waltham, MA). Quantification of cAMP in these lysates was performed using ELISA kit, as per manufacturer's protocol. Data are presented as mean ± SEM of pmol/μg protein from 3 or more batches of dissociated DRG neurons.

2.10. Biochemical assay for Src phosphorylation

Cultured mouse DRG neurons were treated with 20 nM PTHrP or 20 nM PTHrP with 100 nM PP2 or vehicle control for 10 min at 37°C and then lysed with lysis buffer containing 20 mM Tris-HCl, 150 mM NaCl, 1% Triton X-100, 1 mM sodium fluoride, 1 mM phenylmethanesulfonyl fluoride and 1× Protease Inhibitory Cocktail (leupeptin, aprotinin, antipain, and benzamidine-HCl). Lysates were run on a 7.5% SDS-PAGE gel and then transferred to nitrocellulose membranes. Following blocking in 4% non-fat milk in Tris-buffered saline, membranes were probed with either rabbit polyclonal anti-Src (1:1000, Clone 36D10, Cell Signaling, Danvers, MA) or rabbit polyclonal anti-Phospho-Src (1:1000, Tyr416, Cell Signaling) antibodies. Membranes were then washed and incubated with goat anti-rabbit IgG-HRP secondary antibody (1:5000, Antibodies Inc., Davis, CA). Blots were incubated with ECL-Plus reagent (Perkin Elmer, Waltham, MA), and the chemiluminescence signals were captured on X-ray film (Kodak-Biomax, Carestream Health, Rochester, NY). Experiments were repeated in four batches of cultured mouse DRG neuron lysates. Signal intensities of pSrc bands were normalized to the signal intensities of tSrc bands for each individual treatment groups using NIH ImageJ software, and presented as fold-change in pSrc levels upon PTHrP or PTHrP+PP2 treatment conditions.

2.11. Membrane isolation and fractionation

HEK293T cells were cultured and transfected with N-terminal myc-tagged rat TRPV1 in pCMV-Tag-3b and C-terminal YFP-tagged rat PTH1R in pcDNA3.1 (generously provided by Dr. Matthew Mahon, Harvard Medical School) using Lipofectamine 2000 reagent (Life Technologies, Grand Island, NY), as described previously [47]. 42–48 hours after transfection, cells were treated with vehicle or 20 nM PTHrP for 10 min at 37°C, washed twice with phosphate-buffered saline (PBS) and then harvested for use in Minute™ Plasma Membrane Protein Isolation Kit (Invent Biotechnologies) according to the manufacturer's protocol, with minor modifications. All the membrane isolation steps were performed at 4°C. Briefly, harvested cells were lysed with buffer-A by vortexing and then centrifuged at 3,000 rpm for 1 min to pellet the nuclei and cell debris. The supernatant was then centrifuged at 16,000 rpm for 30 min; the resultant supernatant was removed (as cytosolic protein fraction), the pellet was re-suspended and mixed with buffer-B, and then centrifuged further at 10,000 rpm for 5 min. The supernatant was collected in another pre-chilled tube, and the pellet was dissolved in lysis buffer [denoted the organelle membrane (OM) fraction]. Ice-cold PBS was added to the supernatant, mixed by inverting, and was then centrifuged at 18,000 rpm for 90 min to pellet down the plasma membrane (PM) fraction. Normalized

quantities of both OM and PM samples were diluted in SDS resolving sample buffer, size fractionated in 7.5% SDS-PAGE, transferred to nitrocellulose membranes, and immunoblotted with mouse monoclonal anti-myc antibody (1:10 tissue culture supernatant; ATCC, Manassas, VA) and goat anti-mouse IgG-HRP secondary antibody (1:10,000; Antibodies Inc., Davis, CA). Blots were developed with ECL-Plus chemiluminescence reagent (Perkin Elmer, Waltham, MA) on X-ray film (Kodak-Biomax, Carestream Health, Rochester, NY). Experiments were repeated in 4 or more batches of transfected cells.

2.12. Statistical analysis

Data are presented as mean ± SEM. All data pertaining to mouse behavior, ELISA, PKCε translocation, and Ca^{2+} imaging experiments were analyzed for their statistical significance with one-way ANOVA with Dunnett's post-hoc analysis, and/or unpaired Student's T-test. All electrophysiology and biochemical data were analyzed with unpaired Student's T-test. All statistical analyses were conducted using Prism 6 (GraphPad Software, San Diego, CA).

3. RESULTS

3.1. Parathyroid hormone-related peptide induces transient receptor potential vanilloid-1-dependent thermal and mechanical hypersensitivity

Parathyroid hormone-related peptide has been suggested to be critical for the metastasis and subsequent growth of advanced breast and prostate cancer cells [17,45]. The tumorigenic actions of PTHrP are mediated by the activation of its receptor PTH1R, which couples to both $G\alpha_s$- and $G\alpha_q$-coupled receptors in different tissue types [1], leading to downstream activation of protein kinases PKA and PKC. Since activation of PKA and PKC in sensory neurons leads to nociceptor sensitization [6,7,57,63,70], we first tested whether PTHrP had any noxious or algogenic effects on peripheral thermal and mechanical hypersensitivity. A prior study reported the induction of thermal hypersensitivity (~25%, compared to baseline) in mice to high dose of PTHrP (20 μM, i.pl.), injected twice a day for 3 days, which resulted from osteoclastic bone resorption in the paws [61]. However, that study did not determine the acute effects of PTHrP on thermal hypersensitivity. In a recent initiative, the US-NIH advocates that experiments should be conducted on both genders, in order to provide a better validation of experimental observations in rodents [14]. Injection of PTHrP (20 nM, 200 nM, 2 μM, and 20 μM in 10 μL saline; i.pl.) into the hind paws of both male and female C57BL/6 mice led to a significant reduction in paw withdrawal latencies (PWLs) 30 min after injection compared to saline injected controls (Fig. 1), indicating the development of thermal hypersensitivity. In both male and female mice, decreased PWLs in response to 20 nM PTHrP injections recovered to saline-injected levels by 5.5 hours. However, thermal hypersensitivity induced by the injection of 200 nM PTHrP recovered to saline-injected control levels in female, but not male mice by 5.5 hours (Fig. 1). Furthermore, thermal hypersensitivity induced by the injection of 100 nM PTHrP in male mice also persisted at 5.5 hours post-injection (Fig. 1). This suggests that male mice might be more sensitive to the effects of PTHrP on thermal hypersensitivity. PTHrP injection had no significant effect on the PWLs in contralateral hind paws of both male and female mice (Fig. 1). Incomplete recovery of ipsilateral PWLs 24 hours post-injection of 20 μM PTHrP (Fig. 1A) is in line

with a prior report, which suggested that this long-term effect is mediated through enhanced osteoclastic bone resorption in hind paws [61].

We next assessed the effect of PTHrP injection on development of mechanical hypersensitivity in mice by applying increasing strengths of Von Frey hair filaments to the hind paws and counting the number of paw withdrawal responses at baseline, 1, 6 and 24 hours post-injection (Fig. 2A–D). PTHrP injection (2 μM in 10 μL saline, i.pl.) caused significant mechanical hypersensitivity 1 hours after injection, which remained at 6 hours, as compared to saline-injected controls (Fig. 2B, C, E), before completely recovering by 24 hours post-injection (Fig. 2D–E). Similar to our observations on thermal hypersensitivity, increasing dose of PTHrP led to increasing magnitude and duration of mechanical hypersensitivity in both female and male mice (Fig. 2E–F). No significant change was observed in the mechanical sensitivity of contralateral paws of both male and female mice following saline and PTHrP injection (Fig. 2E–F).

Because TRPV1 is highly critical in the development of both inflammatory thermal and mechanical hypersensitivity [10,16,23,53,69,79], we next investigated the requirement of TRPV1 in this context. Consistent with a prior report [49], we found that the mRNA for the PTHrP receptor, PTH1R, is expressed in mouse DRG neurons (Supplemental Fig. 1A). Using double immunofluorescence staining of mouse DRG sections, we found that 82.3 ± 6.4% of TRPV1-positive cells also show PTH1R immunoreactivity, and 35.1% ± 5.6% of PTH1R-positive cells show TRPV1 immunoreactivity (Supplemental Fig. 1B). This suggests that PTH1R protein is co-expressed in a subset of DRG neurons, the vast majority of which express TRPV1. Furthermore, PTHrP-induced (1 μM, in 10 μL saline, i.pl.) thermal and mechanical hypersensitivity were completely absent in both female and male *Trpv1*$^{-/-}$ mice (Fig. 3), suggesting that PTHrP-induced enhancement of cutaneous thermal and mechanical hypersensitivity in mice is dependent on TRPV1.

It has been reported that mice of different genetic background exhibit altered peripheral pain sensitivities [56]. In this line, it must be noted here that although age- and sex-matched same genetic background of mice (C57BL6/J) were used for the comparison of WT vs *Trpv1*$^{-/-}$, no littermate-controlled WT and *Trpv1*$^{-/-}$ mice from the same breeding batch (*Trpv1*$^{+/-}$ × *Trpv1*$^{+/-}$) were used in this study. Also, the difference in the sensitivity of female vs male mice to PTHrP is not clear from our studies. Since the female mice used in these behavioral experiments were not staged for any specific estrous cycle stage(s), influences from different hormones, and from differential bone metabolic effects of PTHrP on relatively low magnitude of thermal and mechanical hypersensitivity in female mice cannot be ruled out.

3.2. Parathyroid hormone-related peptide enhances sensory neuron excitability

We next performed current-clamp recordings on cultured mouse DRG neurons to determine if PTHrP could influence TRPV1-dependent sensory neuron excitability. We found that perfusion of PTHrP (2 nM, 1 min) significantly increased the frequency of capsaicin-evoked (50 nM, 30 s) AP firing (Fig. 4A, D). In these experiments, drug applications were performed locally onto the neuron being recorded, due to which short application (1 min) of a low concentration of PTHrP (2 nM) was sufficient to induce a significant increase in sensitization of AP firing. Since capsaicin is not an endogenous activator of TRPV1, we next

performed these experiments focusing on the proton-activation of TRPV1, a condition analogous to the acidic tumor microenvironment [39]. Perfusion of mild acidic extracellular buffer (pH 6.8; 30 s) under control conditions evoked very few APs, however, perfusion of PTHrP (2 nM, 1 min) led to a significant increase in the frequency of pH 6.8-induced AP firing (Fig. 4B, D). This increase in PTHrP-dependent pH 6.8-induced AP firing frequency was reduced, but not completely abolished in cultured DRG neurons from *Trpv1*$^{-/-}$ mice (Fig. 4C, D). These results suggest that PTHrP at low nanomolar concentrations could lead to constitutive activation of TRPV1 and sensory neuron firing in the mild-to-moderately acidic tumor microenvironment.

We also observed that PTHrP application led to the enhancement of spontaneous AP firing frequency in cultured DRG neurons from both *Trpv1*$^{+/+}$ and *Trpv1*$^{-/-}$ mice (Fig. 4A–C, E). The extent of PTHrP-modulation of spontaneous AP firing was similar, and not significantly different in DRG neurons from *Trpv1*$^{+/+}$ and *Trpv1*$^{-/-}$ mice (Fig. 4E). Furthermore, we calculated the time lag to 1st AP after PTHrP treatment, which is 23.19 ± 4.26 sec and 26.08 ± 5.05 sec in *Trpv1*$^{+/+}$ and *Trpv1*$^{-/-}$ neurons, respectively. Although it could be a matter of debate whether to designate these increased firing as PTHrP-evoked firing or PTHrP-modulation of spontaneous firing, we chose to adapt the later one due to the following reasons: 1) PTHrP did not lead to fast generator potential or membrane depolarization, 2) PTHrP did not not evoke AP firing immediately upon treatment, and 3) A >20 s time lag to 1st AP was observed after PTHrP treatment. Furthermore, spontaneous AP firings were observed in DRG neurons from both mice, without any agonist treatment. Therefore, these data are referred to as “PTHrP-modulation of spontaneous firing” in this study. Since perfusion of PTHrP alone led to modulation of spontaneous AP firing in cultured mouse DRG neurons from both *Trpv1*$^{+/+}$ and *Trpv1*$^{-/-}$ mice (Fig. 4A–C, E), it raises the possibility that PTHrP application might also act on other excitable channels to increase the excitability of DRG neurons. However, with our observation that PTHrP-induced thermal and mechanical hypersensitivity are abolished in *Trpv1*$^{-/-}$ mice (Fig. 3), the contribution of direct PTHrP-modulation of AP firing is highly likely to be minimal.

3.3. Parathyroid hormone-related peptide potentiates transient receptor potential vanilloid-1 channel activity

Because our results showed that PTHrP-induced cutaneous thermal and mechanical hypersensitivity, as well as enhanced sensory neuron firing are largely dependent on TRPV1, we further explored the effects of PTHrP on TRPV1 channel function by utilizing voltage-clamp electrophysiology. Direct perfusion of three consecutive episodes of capsaicin (50 nM, 5 s) to cultured small/medium-diameter DRG neurons (with 1 min extracellular buffer washing in between) led to TRPV1-mediated inward currents that exhibited desensitization during the 2nd and 3rd capsaicin applications (Fig. 5A). Perfusion of PTHrP (2 nM, 1 min) after the 2nd capsaicin application led to a significant increase in TRPV1 current amplitude during the 3rd capsaicin application (Fig. 5A). Similar to current-clamp experiments, drug applications were performed locally onto the neuron being recorded, due to which 1 min application of PTHrP was sufficient to elicit high magnitude of sensitization of TRPV1 activity. Similarly, perfusion of PTHrP (2 nM, 1 min) enhanced the sustained component of pH 6.8-induced inward currents in DRG neurons (Fig. 5B), which is a characteristic of

proton-activated TRPV1 currents [10,11,47]. Such potentiation of pH 6.8-induced sustained inward currents was largely attenuated in cultured DRG neurons from *Trpv1*$^{-/-}$ mice (Fig. 5C). Quantification of peak currents in response to the 3rd vs the 2nd capsaicin application showed a ~7-fold increase in TRPV1 channel activity following PTHrP perfusion (Fig. 5D). Similarly, quantification of the peak sustained component of pH 6.8-induced currents before and after PTHrP application showed an ~11-fold increase in the magnitude of these currents in response to PTHrP, which was attenuated (~1.5-fold increase) in cultured DRG neurons from *Trpv1*$^{-/-}$ mice (Fig. 5D). Additionally, we performed experiments to determine the effect of PTHrP on pH dose-response relationship of sustained inward current activation in mouse DRG neurons. While perfusion of PTHrP (2 nM; 1 min) did not significantly change the EC_{50} of the pH dose-response curve (pH 5.98 ± 0.06 with PTHrP treatment vs. pH 6.04 ± 0.11 for control), we did observe a significant increase in response magnitudes at mild acidic pHs (6.8 and 6.4; Fig. 5E). This observation is highly relevant to the well-known mild-to-moderate acidic tumor microenvironment [39]. We also determined the PTHrP dose-response relationship for modulation of TRPV1 currents by performing experiments as described for Fig. 5A, with increasing concentrations of PTHrP (20 pM, 200 pM, 600 pM, 2 nM, and 20 nM). The EC_{50} for PTHrP-modulation of capsaicin-activated TRPV1 currents was 0.56 nM, with a 95% confidence interval ranging from 0.25 nM to 1.26 nM (Fig. 5F). Significant TRPV1 current modulation could be observed with PTHrP concentrations as low as 200 pM. Taken together, these results suggest that elevated levels of PTHrP, in combination with the acidic tumor microenvironment could lead to constitutive activation of TRPV1 on adjacent sensory afferents, resulting in enhanced neuronal firing and induction of thermal and mechanical hypersensitivity.

3.4. Parathyroid hormone-related peptide-mediated sensitization of transient receptor potential vanilloid-1 is dependent on protein kinase C activation

PTH1R is a G-protein coupled receptor (GPCR), which upon activation by PTHrP results in downstream activation of PKA and/or PKC in different tissue types [1]. Our results show that PTH1R is expressed in the vast majority of TRPV1-expressing DRG neurons in mice (Supplemental Fig. 1). We next tested whether PTHrP treatment could lead to the activation of PKC and/or PKA in mouse DRG neurons. Upon activation, several isoforms of PKC, mainly PKCε, PKCβ, and PKCδ translocate towards the plasma membrane [12,29,47]. Treatment of cultured mouse DRG neurons with PTHrP (20 nM for 5, 15 and 30 min) significantly increased the magnitude and number of neurons exhibiting PKCε translocation to the cell periphery (Fig. 6A–B). PMA, a direct activator of PKC, was used as a positive control in these experiments, which showed robust PKCε translocation to the cell periphery (Fig. 6A–B). Next, we verified whether PKA could also be activated in DRG neurons upon PTHrP treatment. PKA activation results from elevated cAMP levels via activation of adenylate cyclase by dissociated $G\alpha_s$ subunits of GPCRs, due to which measurement of cellular cAMP levels serves as an indirect measurement of PKA activity [80]. Treatment of mouse DRG neurons with forskolin (10 μM, 5 min), a direct activator of adenylate cyclases, increased cAMP levels measured by ELISA (Fig. 6C). However, PTHrP treatment (20 nM for 5, 15 and 30 min) did not lead to any significant increase in the cAMP levels, compared to untreated control conditions (Fig. 6C), suggesting that PTH1R could presumably signal through a $G\alpha_q$,-coupled downstream signaling pathway in mouse DRG neurons. The other

parathyroid hormone receptor, PTH2R, has also been reported to be expressed in myelinated nociceptive DRG neurons in mice [52]. PTH2R is expressed as a functional $G\alpha_q$,-coupled receptor in mouse DRG neurons, wherein activation by its specific agonist, tuberoinfundibular peptide-39, leads to increased cAMP production and PKA activation [52]. Since PTHrP has no significant binding activity on PTH2R, rather it specifically activates PTH1R [25], and that our results show no significant cAMP production in mouse DRG neurons, it is highly unlikely that PTH2R plays any significant role in mediating PTHrP effects.

We next functionally verified the specific kinase involvement in PTHrP-mediated potentiation of TRPV1 currents. In agreement with electrophysiological results, we utilized functional Ca^{2+} imaging to show that PTHrP (20 nM, 5 min) significantly enhanced capsaicin-evoked Ca^{2+} influx in cultured mouse DRG neurons (Fig. 6D). In these experiments, drug applications were performed globally on the entire recording chamber, due to which relatively longer application (5 min) of 10-fold high concentration of PTHrP (20 nM) was given, as compared to electrophysiological experiments. This potentiation of Ca^{2+} influx was attenuated by co-application of PTHrP with the PKC inhibitor BIM-I (1 μM) in DRG neurons from both female and male mice (Fig. 6E–F). However, co-application of the PKA inhibitor KT5720 (1 μM) failed to attenuate the PTHrP-mediated potentiation of capsaicin-evoked Ca^{2+} influx (Fig. 6E–F), consistent with our observations from PKC and PKA activation assays in mouse DRG neurons treated with PTHrP.

We also quantified the proportion of neurons that exhibit significant sensitization of TRPV1-mediated Ca^{2+} influx after exposure to PTHrP, by taking into account the proportion of neurons that exhibited ≥90% of peak Ca^{2+} responses to 2nd capsaicin vs 1st capsaicin application. Under our experimental conditions, ~25 to 40% of cultured DRG neurons exhibit capsaicin-induced Ca^{2+} flux, which is in good agreement with the percent of functional TRPV1-positive DRG neurons in C57BL/6 mice widely reported in the literature. PTHrP application resulted in 77.6% of capsaicin-responsive neurons exhibiting significant sensitization of TRPV1-mediated Ca^{2+} influx, as opposed to 9.6% of capsaicin-responsive neurons in control conditions (n = >100 neurons from >10 batch of neuron cultures for each group). This is in good agreement with our observations from mouse DRG section immunostaining (Supplemental Fig. 1B), where 82.3 ± 6.4% of TRPV1-positive cells show PTH1R immunoreactivity.

3.5. Parathyroid hormone-related peptide enhances the proportion of capsaicin-responsive DRG neurons and is dependent on protein kinase C and Src kinase activity

While performing Ca^{2+} imaging experiments on PTHrP-modulation of TRPV1, we made an interesting observation. A significant proportion of cultured mouse DRG neurons (~22% of all neurons imaged) that did not elicit any Ca^{2+} influx in response to capsaicin application became capsaicin-responsive upon PTHrP (20 nM, 5 min) exposure (~1% neurons in control/wash condition vs ~22% neurons in PTHrP application; Fig. 7A–B). This phenomenon is referred to as the recruitment of non-capsaicin-responsive neurons to become capsaicin-responsive. Since our results show that inhibition of PKC attenuated PTHrP-induced sensitization of TRPV1 channel activation (Fig. 6E–F), we next tested if

PKC activity could also influence the recruitment of capsaicin-responsive neurons by PTHrP application. Co-application of the PKC inhibitor BIM-I (1 μM), but not the PKA inhibitor KT5720 (100 nM) led to significant attenuation of PTHrP-induced recruitment of capsaicin-responsive DRG neurons (Fig. 7B). Previous studies have shown that Src kinase can be activated downstream of PKC, resulting in phosphorylation of TRPV1 at the residue Y200, which could ultimately lead to increased surface delivery of TRPV1 protein to the plasma membrane [37,87]. Accordingly, we observed that co-application of the Src kinase inhibitor PP2 (100 nM) significantly attenuated the PTHrP-induced recruitment of capsaicin-responsive neurons (Fig. 7B). PP2 has been suggested to have significant inhibitory effects on other kinases *in vitro* at higher concentrations, such as ~10 μM or more [9]. Although in our studies we utilized PP2 at nanomolar concentrations for its effective inhibitory activity on Src, we next verified the specificity of Src activity in PTHrP-induced recruitment of capsaicin-responsive neurons by expressing dominant-negative Src (DN-Src) in cultured mouse DRG neurons. PTHrP application led to the recruitment of 19.75 ± 3.1% capsaicin-responsive neurons that were transfected with only GFP, similar to that observed for control un-transfected neurons (Fig. 7A–B). This indicated that nucleofection of mouse DRG neurons did not adversely affect PTHrP-induced recruitment of capsaicin-responsive neurons. In contrast, PTHrP-induced recruitment of capsaicin-responsive neurons was attenuated in neurons transfected with DN-Src (Fig. 7B), suggesting that the inhibitory effects of PP2 on PTHrP-induced recruitment of capsaicin-responsive neurons is highly likely to be mediated via inhibition of Src activity. However, inhibition of Src did not lead to the attenuation of PTHrP-induced sensitization of TRPV1 activation by capsaicin (Fig. 7C), suggesting that Src activity mainly influences the recruitment of capsaicin-responsive neurons by PTHrP.

To support our observation on the role of Src, we verified that levels of phosphorylated (activated) Src (p-Src) were increased upon PTHrP exposure (20 nM, 5 min) in cultured mouse DRG neurons, which was reduced by co-application of PP2 (100 nM; Fig. 8A–B). To further strengthen our observation on Src-dependent recruitment of capsaicin-responsive neurons, we next investigated if PTHrP-mediated Src phosphorylation indeed leads to an increase in TRPV1 protein levels in the plasma membrane. Cellular membrane fractionation assay were performed in HEK293T cells transfected with either recombinant rat TRPV1-myc-WT or TRPV1-myc-Y199F (equivalent to Y200 in mouse TRPV1 as the Src phosphorylation site) along with rat PTH1R-YFP constructs and treated with PTHrP (20 nM, 10 min). A significant increase in the plasma membrane TRPV1-WT protein levels was observed upon PTHrP treatment, whereas no such increase was observed for TRPV1-Y199F after PTHrP treatment (Fig. 8C–D). Overall, these results suggest that PTHrP-mediated activation of PKC leads to the sensitization of TRPV1 channel activity. In addition, downstream PKC-mediated activation of Src leads to an increase in the number of TRPV1 channels on plasma membrane, which presumably results in an increase in the proportion of neurons that now express functional TRPV1 on the plasma membrane and undergo sensitization upon PTHrP exposure.

3.6. Parathyroid hormone-related peptide-induced thermal hypersensitivity is dependent on protein kinase C and Src

Because increased PKC and Src activity underlie the modifications in TRPV1 function and trafficking in cultured mouse DRG neurons, we next asked whether they are critical to PTHrP-induced thermal and mechanical hypersensitivity in mice. Co-injection (i.pl.) of PTHrP with the inhibitors for PKC (BIM-I, 10 μg) or Src (PP2, 3 μg) attenuated thermal hypersensitivity in both female (Fig. 9A–B) and male (Fig. 9D–E) mice. Interestingly, co-injection of PP2 failed to attenuate PTHrP-induced (200 nM) mechanical hypersensitivity (Fig. 9C, F). Since 200 nM PTHrP elicits only a modest increase in mechanical hypersensitivity, we also performed these experiments with 1 μM PTHrP, wherein PP2 failed to attenuate a stronger mechanical hypersensitivity (Fig. 9C). Injection of PP2 alone did not lead to any change in thermal and mechanical hypersensitivity, as compared to saline injected controls. Similarly, co-injection of BIM-I failed to attenuate PTHrP-induced (200 nM) mechanical hypersensitivity (not shown). Altogether, these results suggest that PKC- and Src-mediated upregulation of TRPV1 are critical to PTHrP-induced thermal, but not mechanical hypersensitivity.

4. DISCUSSION

The results from our study suggest that PTHrP significantly enhances both peripheral thermal and mechanical hypersensitivity in mice, which is dependent on functional expression of TRPV1. These effects of PTHrP are linked to PKC-mediated potentiation of TRPV1 channel function on sensory neurons, resulting in enhanced AP firing. In addition, PTHrP exposure results in an increase in TRPV1 trafficking to the plasma membrane, and increased proportion of DRG neurons that functionally respond to channel activators. Consistent with these observations, PTHrP-induced thermal hypersensitivity was attenuated by PKC and Src inhibitors. Together, our findings demonstrate that PTHrP, which plays a key role in both cancer metastasis and subsequent tumor growth in breast and prostate cancer, could also play a critical role in sensory afferent excitation and firing mainly via upregulation of TRPV1 function and trafficking, along with the acidic tumor microenvironment. This could presumably serve as a molecular and cellular mechanism underlying peripheral detection and transmission of pain-producing stimuli in metastatic cancers.

Although it is largely accepted that there are sex differences in the magnitude and perception of pain, very few rodent studies use mice of both genders [18,55,60]. Some studies have suggested that female mice are more sensitive to noxious/painful stimuli, whereas other studies have ruled out any sex differences in pain perception [5,84]. Since PTHrP is critical in rodent metastasis studies in both breast and prostate cancers [45,67], we chose to determine its role in pain induction in both female and male mice. Our results show relatively long-lasting PTHrP-induced thermal hypersensitivity in male mice compared to females. This could be due to differential expression of PTH1R and/or TRPV1 in different subsets of sensory neurons in male vs female sensory neurons. Also the role of specific hormones in estrous cycle stages and the role of PTHrP in metabolism contributing to reduced pain sensitivity in female mice could not be completely ruled out. Interestingly, our

results show no gender-related differences in PKC/Src-modulation of TRPV1 in mouse DRG neurons. Therefore, further studies are needed to delineate these differences at cellular, molecular and hormonal levels. Nevertheless, our study suggests that PTHrP could serve as a common modulator of peripheral sensory afferent excitation and pain associated with advanced breast and prostate cancers.

Parathyroid hormone-related peptide did not induce any change in thermal and mechanical sensitivity of *Trpv1*$^{-/-}$ mice, suggesting the critical role of TRPV1. PTHrP-sensitization of mild acidic pH-induced AP firing frequency and the magnitude of sustained inward currents were reduced in *Trpv1*$^{-/-}$ DRG neurons. However, the enhanced spontaneous AP firing frequency in response to PTHrP was of similar magnitude in both *Trpv1*$^{+/+}$ and *Trpv1*$^{-/-}$ DRG neurons, suggesting that other sensory ion channel(s) might undergo activation/modulation to increase neuronal excitability. The residual potentiating effects of PTHrP on proton-induced sustained inward currents in *Trpv1*$^{-/-}$ mice might be a consequence of PKC modulation of acid-sensing ion channels (ASICs), specifically ASIC3 [13]. Additionally, the role of major sensory voltage-gated Na^+ (Na_V) channels, $Na_V1.7$ and $Na_V1.8$, in PTHrP-induced enhancement of DRG neuron excitability cannot be ruled out, since these channels also undergo functional modulation by PKC and Src [2]. PTHrP could also influence the function of voltage-gated Ca^{2+} (Ca_V) and K^+ (K_V) channels that are expressed in mouse DRG neurons [8,85], thereby influencing the excitability of these neurons. PKC phosphorylation of $K_V4.2$ downregulates channel function in hippocampal neurons, leading to increased neuronal excitability [26]. Since $K_V4.2$ channel is also expressed in DRG neurons [85], a similar mechanism could also contribute to PTHrP-induced enhancement of neuronal excitability. Future in-depth investigations are therefore required to identify and characterize the modulation of function and/or trafficking of these excitable and other nociceptive channels by PTHrP that enhance AP firing in DRG neurons. Nevertheless, our results show that PTHrP-induced increase in peripheral pain sensitivity is absent in *Trpv1*$^{-/-}$ mice, implicating TRPV1 as the critical initiator/regulator.

Importantly, our study shows that PTHrP can potentiate TRPV1 at concentrations as low as ~200 pM. Human patients with bone-metastasized breast cancers have elevated levels of PTHrP in plasma at a similar level [82], although PTHrP levels could be much higher in the metastatic bone tumor microenvironment. In addition, the acidic microenvironment of bone-metastasized tumors could provide a favorable condition for constitutive activation of TRPV1 and sustained AP firing, thereby inducing peripheral transmission of painful signals in these pathologies. Our results show PTH1R expression in TRPV1-positive sensory neurons in L4–L6 mouse DRGs that innervate the hind limb bones [36], wherein TRPV1 has also been shown to be expressed on CGRP-positive sensory afferents [77]. PTHrP has been shown to be critical for tumor-induced increase in osteoclast activity [61,86] that constitutes a significant source of the elevated levels of G-CSF/GM-CSF, which also sensitize TRPV1 and nociceptive afferents [76,81]. Therefore, modulation of TRPV1 on bone sensory afferents by convergent signaling pathways initiated by PTHrP could constitute a mechanism for peripheral pain sensitization in advanced breast and prostate cancers. In fact, TRPV1 has already been implicated in mouse sarcoma models of bone cancer pain [21,51]. The TRPV1 antagonist ABT-102, which effectively attenuates proton-activation of the channel without eliciting significant hyperthermia [27,64], could therefore serve as an attractive candidate for

alleviation of chronic pain associated with bone-metastasized breast and prostate cancers in pre-clinical settings.

It is well established that inflammatory mediators such as bradykinin, NGF, LPA, and C-type natriuretic peptide activate PKC, leading to sensitization of TRPV1 function and an increase in thermal hypersensitivity [28,47,65]. Here we show that PTHrP is another such modulator and exerts similar effects on TRPV1. Interestingly, PTHrP induces both thermal and mechanical hypersensitivity, which are absent in *Trpv1*$^{-/-}$ mice. So far, the relationship between TRPV1 and mechanical sensitivity is poorly understood. Early studies showed no change in mechanical hypersensitivity in *Trpv1*$^{-/-}$ compared to wild-type mice after inflammation [10]. However, subsequent studies in mouse models of inflammation, bone sarcoma, sickle cell disease, and nerve injury implicate TRPV1 as an important mediator of mechanical hypersensitivity [23,53,69,79], although the underlying mechanism(s) remains un-elucidated. We show that PTHrP-induced mechanical hypersensitivity is absent in *Trpv1*$^{-/-}$ mice. However, Src and PKC inhibitors were unable to attenuate such mechanical hypersensitivity in wild-type mice. This suggests that TRPV1 is presumably a critical initiator, but not direct transducer of PTHrP-mediated mechanical hypersensitivity, and phospho-modulation of TRPV1 by PKC/Src is only critical for thermal, but not mechanical hypersensitivity.

Activation of multiple kinases, such as PKA, PKC, and MAPK by various pro-/inflammatory mediators, growth factors and bioactive peptides phosphorylate TRPV1, which is critical for the development of thermal hyperalgesia [22,38,44,71]. Although Src phosphorylation upregulates the proportion of TRPV1 on plasma membrane, its role in thermal hyperalgesia was not established [33,37,87]. Interestingly, a previous study showed that mice deficient in c-Src exhibit reduced CFA-induced thermal hypersensitivity compared to wild-type mice [61]. Our results show that inhibition of PKC/Src attenuated PTHrP-induced thermal hypersensitivity. Also, PKC inhibition blocked both PTHrP-sensitization of TRPV1 function and recruitment of functional TRPV1-responsive neurons, whereas Src inhibition only blocked the latter, indicating that Src activation is downstream of PKC, as suggested before [87]. Since Src inhibition alone is sufficient to attenuate PTHrP-induced thermal hypersensitivity, enhanced TRPV1 trafficking could therefore be an important mechanism underlying the development of thermal hypersensitivity. Indeed, reports utilizing single fiber recordings from intact nerve fiber preparations showed a significant increase in functional TRPV1-positive cutaneous afferent numbers after inflammation [40]. Further studies investigating the role of Src-dependent recruitment of TRPV1 in mouse models of neuropathic and cancer pain models could suggest the therapeutic targeting of such a mechanism for multiple pain pathologies. It has also been reported that the A-kinase anchoring protein-5 (AKAP5) physically interacts with TRPV1, as well as with PKC and PKA, thereby providing the sensory neurons with a local signalosome for the phospho-modulation of TRPV1. In fact, competitive targeting of AKAP5 interaction with PKC or PKA or TRPV1 has been shown to attenuate thermal hypersensitivity in experimental mouse models [19,32,34,70,75]. Since our results show the critical role for Src-induced TRPV1 trafficking in PTHrP-induced thermal hypersensitivity, it would be attractive to further investigate the role of AKAP5 therein.

Src influences the metastasis of several cancers, including breast and prostate [72,73,83,88]. In mouse models, Src inhibition attenuated breast cancer bone metastasis [74,88]. Src is also critical for osteoclast activity, which contributes to metastatic bone tumor growth, as well as in pain associated with these metastases [54,61]. Nociceptor sensitization by tumor-enriched factors, G-CSF and GM-CSF, has also been suggested to be mediated in part via increased Src activity [76,81]. Therefore Src could constitute a common target for the treatment and/or prevention of metastatic bone tumors, as well as the associated chronic pain.

In summary, our study shows that PKC and Src activity are critical to PTHrP-induced modulation of TRPV1 function and trafficking. This, in combination with the acidic microenvironment and high levels of PTHrP in metastatic cancers, could sub-serve a mechanism for enhanced sensory nerve excitation and chronic pain associated with advanced breast and prostate cancers. Also, our study describes an important role for Src-mediated trafficking of TRPV1 in the development of thermal nociception, which could likely have a large influence on a variety of painful pathologies.

Supplementary Material

Refer to Web version on PubMed Central for supplementary material.

Acknowledgments

This work was supported by NIH grants NINDS-NS069898 (to DPM), NCI-F31-CA171927, and NIGMS-T32-NS045549 (to ADM), US Department of Defense (DoD) Prostate Cancer Research Program IDEA grant PC101096 (to DPM), and start-up funds from the Washington University School of Medicine, Department of Anesthesiology and Washington University Pain Center (to DPM). The funders of this study did not have any influence on the study design, data collection and decision to publish the experimental observations.

The authors wish to thank Drs. Donna L. Hammond, Yuriy M. Usachev and Christopher J. Benson (University of Iowa Carver College of Medicine), as well as Dr. Robert W. Gereau IVth for their critical suggestions in this work. The plasmid containing rat TRPV1 cDNA was generously provided by Dr. David J. Julius. The plasmid pcDNA3 carrying DN-Src was previously generated by incorporating K297M and Y529F mutations in mouse Src cDNA. (generously provided by Dr Johannes W. Hell).

References

1. Abou-Samra AB, Juppner H, Force T, Freeman MW, Kong XF, Schipani E, Urena P, Richards J, Bonventre JV, Potts JT Jr, et al. Expression cloning of a common receptor for parathyroid hormone and parathyroid hormone-related peptide from rat osteoblast-like cells: a single receptor stimulates intracellular accumulation of both cAMP and inositol trisphosphates and increases intracellular free calcium. Proceedings of the National Academy of Sciences of the United States of America. 1992; 89(7):2732–2736. [PubMed: 1313566]
2. Amir R, Argoff CE, Bennett GJ, Cummins TR, Durieux ME, Gerner P, Gold MS, Porreca F, Strichartz GR. The role of sodium channels in chronic inflammatory and neuropathic pain. The journal of pain : official journal of the American Pain Society. 2006; 7(5 Suppl 3):S1–29.
3. Andratsch M, Mair N, Constantin CE, Scherbakov N, Benetti C, Quarta S, Vogl C, Sailer CA, Uceyler N, Brockhaus J, Martini R, Sommer C, Zeilhofer HU, Muller W, Kuner R, Davis JB, Rose-John S, Kress M. A key role for gp130 expressed on peripheral sensory nerves in pathological pain. The Journal of neuroscience : the official journal of the Society for Neuroscience. 2009; 29(43): 13473–13483. [PubMed: 19864560]
4. Asai H, Ozaki N, Shinoda M, Nagamine K, Tohnai I, Ueda M, Sugiura Y. Heat and mechanical hyperalgesia in mice model of cancer pain. Pain. 2005; 117(1–2):19–29. [PubMed: 16043290]

5. Banik RK, Woo YC, Park SS, Brennan TJ. Strain and sex influence on pain sensitivity after plantar incision in the mouse. Anesthesiology. 2006; 105(6):1246–1253. [PubMed: 17122588]
6. Bhave G, Hu HJ, Glauner KS, Zhu W, Wang H, Brasier DJ, Oxford GS, Gereau RW IV. Protein kinase C phosphorylation sensitizes but does not activate the capsaicin receptor transient receptor potential vanilloid 1 (TRPV1). Proceedings of the National Academy of Sciences. 2003; 100(21): 12480–12485.
7. Bhave G, Zhu W, Wang H, Brasier DJ, Oxford GS, Gereau RW IV. cAMP-Dependent Protein Kinase Regulates Desensitization of the Capsaicin Receptor (VR1) by Direct Phosphorylation. Neuron. 2002; 35(4):721–731. [PubMed: 12194871]
8. Bourinet E, Altier C, Hildebrand ME, Trang T, Salter MW, Zamponi GW. Calcium-permeable ion channels in pain signaling. Physiological reviews. 2014; 94(1):81–140. [PubMed: 24382884]
9. Brandvold KR, Steffey ME, Fox CC, Soellner MB. Development of a highly selective c-Src kinase inhibitor. ACS chemical biology. 2012; 7(8):1393–1398. [PubMed: 22594480]
10. Caterina MJ, Leffler A, Malmberg AB, Martin WJ, Trafton J, Petersen-Zeitz KR, Koltzenburg M, Basbaum AI, Julius D. Impaired nociception and pain sensation in mice lacking the capsaicin receptor. Science. 2000; 288(5464):306–313. [PubMed: 10764638]
11. Caterina MJ, Schumacher MA, Tominaga M, Rosen TA, Levine JD, Julius D. The capsaicin receptor: a heat-activated ion channel in the pain pathway. Nature. 1997; 389(6653):816–824. [PubMed: 9349813]
12. Cesare P, Dekker LV, Sardini A, Parker PJ, McNaughton PA. Specific involvement of PKC-epsilon in sensitization of the neuronal response to painful heat. Neuron. 1999; 23(3):617–624. [PubMed: 10433272]
13. Chu XP, Papasian CJ, Wang JQ, Xiong ZG. Modulation of acid-sensing ion channels: molecular mechanisms and therapeutic potential. International journal of physiology, pathophysiology and pharmacology. 2011; 3(4):288–309.
14. Clayton JA, Collins FS. Policy: NIH to balance sex in cell and animal studies. Nature. 2014; 509(7500):282–283. [PubMed: 24834516]
15. Constantin CE, Mair N, Sailer CA, Andratsch M, Xu ZZ, Blumer MJ, Scherbakov N, Davis JB, Bluethmann H, Ji RR, Kress M. Endogenous tumor necrosis factor alpha (TNFalpha) requires TNF receptor type 2 to generate heat hyperalgesia in a mouse cancer model. The Journal of neuroscience : the official journal of the Society for Neuroscience. 2008; 28(19):5072–5081. [PubMed: 18463260]
16. Davis JB, Gray J, Gunthorpe MJ, Hatcher JP, Davey PT, Overend P, Harries MH, Latcham J, Clapham C, Atkinson K, Hughes SA, Rance K, Grau E, Harper AJ, Pugh PL, Rogers DC, Bingham S, Randall A, Sheardown SA. Vanilloid receptor-1 is essential for inflammatory thermal hyperalgesia. Nature. 2000; 405(6783):183–187. [PubMed: 10821274]
17. Deftos LJ, Barken I, Burton DW, Hoffman RM, Geller J. Direct evidence that PTHrP expression promotes prostate cancer progression in bone. Biochemical and biophysical research communications. 2005; 327(2):468–472. [PubMed: 15629138]
18. Fillingim RB, King CD, Ribeiro-Dasilva MC, Rahim-Williams B, Riley JL 3rd. Sex, gender, and pain: a review of recent clinical and experimental findings. The journal of pain : official journal of the American Pain Society. 2009; 10(5):447–485. [PubMed: 19411059]
19. Fischer MJ, Btesh J, McNaughton PA. Disrupting sensitization of transient receptor potential vanilloid subtype 1 inhibits inflammatory hyperalgesia. The Journal of neuroscience : the official journal of the Society for Neuroscience. 2013; 33(17):7407–7414. [PubMed: 23616546]
20. Gach K, Wyrebska A, Fichna J, Janecka A. The role of morphine in regulation of cancer cell growth. Naunyn-Schmiedeberg's archives of pharmacology. 2011; 384(3):221–230.
21. Ghilardi JR, Rohrich H, Lindsay TH, Sevcik MA, Schwei MJ, Kubota K, Halvorson KG, Poblete J, Chaplan SR, Dubin AE, Carruthers NI, Swanson D, Kuskowski M, Flores CM, Julius D, Mantyh PW. Selective blockade of the capsaicin receptor TRPV1 attenuates bone cancer pain. The Journal of neuroscience : the official journal of the Society for Neuroscience. 2005; 25(12):3126–3131. [PubMed: 15788769]
22. Gold MS, Gebhart GF. Nociceptor sensitization in pain pathogenesis. Nature medicine. 2010; 16(11):1248–1257.

23. Hillery CA, Kerstein PC, Vilceanu D, Barabas ME, Retherford D, Brandow AM, Wandersee NJ, Stucky CL. Transient receptor potential vanilloid 1 mediates pain in mice with severe sickle cell disease. Blood. 2011; 118(12):3376–3383. [PubMed: 21708890]
24. Hirth M, Rukwied R, Gromann A, Turnquist B, Weinkauf B, Francke K, Albrecht P, Rice F, Hagglof B, Ringkamp M, Engelhardt M, Schultz C, Schmelz M, Obreja O. Nerve growth factor induces sensitization of nociceptors without evidence for increased intraepidermal nerve fiber density. Pain. 2013; 154(11):2500–2511. [PubMed: 23891896]
25. Hoare SR, Usdin TB. Molecular mechanisms of ligand recognition by parathyroid hormone 1 (PTH1) and PTH2 receptors. Current pharmaceutical design. 2001; 7(8):689–713. [PubMed: 11375776]
26. Hoffman DA, Johnston D. Downregulation of transient K+ channels in dendrites of hippocampal CA1 pyramidal neurons by activation of PKA and PKC. The Journal of neuroscience : the official journal of the Society for Neuroscience. 1998; 18(10):3521–3528. [PubMed: 9570783]
27. Honore P, Chandran P, Hernandez G, Gauvin DM, Mikusa JP, Zhong C, Joshi SK, Ghilardi JR, Sevcik MA, Fryer RM, Segreti JA, Banfor PN, Marsh K, Neelands T, Bayburt E, Daanen JF, Gomtsyan A, Lee CH, Kort ME, Reilly RM, Surowy CS, Kym PR, Mantyh PW, Sullivan JP, Jarvis MF, Faltynek CR. Repeated dosing of ABT-102, a potent and selective TRPV1 antagonist, enhances TRPV1-mediated analgesic activity in rodents, but attenuates antagonist-induced hyperthermia. Pain. 2009; 142(1–2):27–35. [PubMed: 19135797]
28. Huang J, Zhang X, McNaughton PA. Inflammatory pain: the cellular basis of heat hyperalgesia. Current neuropharmacology. 2006; 4(3):197–206. [PubMed: 18615146]
29. Hucho TB, Dina OA, Levine JD. Epac mediates a cAMP-to-PKC signaling in inflammatory pain: an isolectin B4(+) neuron-specific mechanism. The Journal of neuroscience : the official journal of the Society for Neuroscience. 2005; 25(26):6119–6126. [PubMed: 15987941]
30. Iddon J, Bundred NJ, Hoyland J, Downey SE, Baird P, Salter D, McMahon R, Freemont AJ. Expression of parathyroid hormone-related protein and its receptor in bone metastases from prostate cancer. The Journal of pathology. 2000; 191(2):170–174. [PubMed: 10861577]
31. Isowa S, Shimo T, Ibaragi S, Kurio N, Okui T, Matsubara K, Hassan NM, Kishimoto K, Sasaki A. PTHrP regulates angiogenesis and bone resorption via VEGF expression. Anticancer research. 2010; 30(7):2755–2767. [PubMed: 20683010]
32. Jeske NA, Diogenes A, Ruparel NB, Fehrenbacher JC, Henry M, Akopian AN, Hargreaves KM. A-kinase anchoring protein mediates TRPV1 thermal hyperalgesia through PKA phosphorylation of TRPV1. Pain. 2008; 138(3):604–616. [PubMed: 18381233]
33. Jeske NA, Patwardhan AM, Henry MA, Milam SB. Fibronectin stimulates TRPV1 translocation in primary sensory neurons. Journal of neurochemistry. 2009; 108(3):591–600. [PubMed: 19012739]
34. Jeske NA, Patwardhan AM, Ruparel NB, Akopian AN, Shapiro MS, Henry MA. A-kinase anchoring protein 150 controls protein kinase C-mediated phosphorylation and sensitization of TRPV1. Pain. 2009; 146(3):301–307. [PubMed: 19767149]
35. Ji RR, Samad TA, Jin SX, Schmoll R, Woolf CJ. p38 MAPK activation by NGF in primary sensory neurons after inflammation increases TRPV1 levels and maintains heat hyperalgesia. Neuron. 2002; 36(1):57–68. [PubMed: 12367506]
36. Jimenez-Andrade JM, Bloom AP, Stake JI, Mantyh WG, Taylor RN, Freeman KT, Ghilardi JR, Kuskowski MA, Mantyh PW. Pathological sprouting of adult nociceptors in chronic prostate cancer-induced bone pain. The Journal of neuroscience : the official journal of the Society for Neuroscience. 2010; 30(44):14649–14656. [PubMed: 21048122]
37. Jin X, Morsy N, Winston J, Pasricha PJ, Garrett K, Akbarali HI. Modulation of TRPV1 by nonreceptor tyrosine kinase, c-Src kinase. American journal of physiology Cell physiology. 2004; 287(2):C558–563. [PubMed: 15084474]
38. Julius D. TRP channels and pain. Annual review of cell and developmental biology. 2013; 29:355–384.
39. Kingsley LA, Fournier PG, Chirgwin JM, Guise TA. Molecular biology of bone metastasis. Molecular cancer therapeutics. 2007; 6(10):2609–2617. [PubMed: 17938257]
40. Koerber HR, McIlwrath SL, Lawson JJ, Malin SA, Anderson CE, Jankowski MP, Davis BM. Cutaneous C-polymodal fibers lacking TRPV1 are sensitized to heat following inflammation, but

fail to drive heat hyperalgesia in the absence of TPV1 containing Cheat fibers. Molecular pain. 2010; 6:58. [PubMed: 20858240]

41. Kondo H, Guo J, Bringhurst FR. Cyclic adenosine monophosphate/protein kinase A mediates parathyroid hormone/parathyroid hormone-related protein receptor regulation of osteoclastogenesis and expression of RANKL and osteoprotegerin mRNAs by marrow stromal cells. Journal of bone and mineral research : the official journal of the American Society for Bone and Mineral Research. 2002; 17(9):1667–1679.
42. Koplas PA, Rosenberg RL, Oxford GS. The role of calcium in the desensitization of capsaicin responses in rat dorsal root ganglion neurons. The Journal of neuroscience : the official journal of the Society for Neuroscience. 1997; 17(10):3525–3537. [PubMed: 9133377]
43. Kozlow W, Guise TA. Breast cancer metastasis to bone: mechanisms of osteolysis and implications for therapy. Journal of mammary gland biology and neoplasia. 2005; 10(2):169–180. [PubMed: 16025223]
44. Kuner R. Central mechanisms of pathological pain. Nature medicine. 2010; 16(11):1258–1266.
45. Li J, Karaplis AC, Huang DC, Siegel PM, Camirand A, Yang XF, Muller WJ, Kremer R. PTHrP drives breast tumor initiation, progression, and metastasis in mice and is a potential therapy target. The Journal of clinical investigation. 2011; 121(12):4655–4669. [PubMed: 22056386]
46. Liao J, Li X, Koh AJ, Berry JE, Thudi N, Rosol TJ, Pienta KJ, McCauley LK. Tumor expressed PTHrP facilitates prostate cancer-induced osteoblastic lesions. International journal of cancer Journal international du cancer. 2008; 123(10):2267–2278. [PubMed: 18729185]
47. Loo L, Shepherd AJ, Mickle AD, Lorca RA, Shutov LP, Usachev YM, Mohapatra DP. The C-type natriuretic peptide induces thermal hyperalgesia through a noncanonical Gbetagamma-dependent modulation of TRPV1 channel. The Journal of neuroscience : the official journal of the Society for Neuroscience. 2012; 32(35):11942–11955. [PubMed: 22933780]
48. Lozano-Ondoua AN, Symons-Liguori AM, Vanderah TW. Cancer-induced bone pain: Mechanisms and models. Neuroscience letters. 2013; 557(Pt A):52–59. [PubMed: 24076008]
49. Macica CM, Liang G, Lankford KL, Broadus AE. Induction of parathyroid hormone-related peptide following peripheral nerve injury: role as a modulator of Schwann cell phenotype. Glia. 2006; 53(6):637–648. [PubMed: 16470617]
50. Mantyh P. Bone cancer pain: causes, consequences, and therapeutic opportunities. Pain. 2013; 154(Suppl 1):S54–62. [PubMed: 23916671]
51. Mantyh PW. Bone cancer pain: from mechanism to therapy. Current opinion in supportive and palliative care. 2014; 8(2):83–90. [PubMed: 24792411]
52. Matsumoto M, Kondo S, Usdin TB, Ueda H. Parathyroid hormone 2 receptor is a functional marker of nociceptive myelinated fibers responsible for neuropathic pain. Journal of neurochemistry. 2010; 112(2):521–530. [PubMed: 19891737]
53. McGaraughty S, Chu KL, Brown BS, Zhu CZ, Zhong C, Joshi SK, Honore P, Faltynek CR, Jarvis MF. Contributions of central and peripheral TRPV1 receptors to mechanically evoked and spontaneous firing of spinal neurons in inflamed rats. Journal of neurophysiology. 2008; 100(6): 3158–3166. [PubMed: 18829846]
54. Miyazaki T, Sanjay A, Neff L, Tanaka S, Horne WC, Baron R. Src kinase activity is essential for osteoclast function. The Journal of biological chemistry. 2004; 279(17):17660–17666. [PubMed: 14739300]
55. Mogil JS. Sex differences in pain and pain inhibition: multiple explanations of a controversial phenomenon. Nature reviews Neuroscience. 2012; 13(12):859–866.
56. Mogil JS, Wilson SG, Bon K, Lee SE, Chung K, Raber P, Pieper JO, Hain HS, Belknap JK, Hubert L, Elmer GI, Chung JM, Devor M. Heritability of nociception I: responses of 11 inbred mouse strains on 12 measures of nociception. Pain. 1999; 80(1–2):67–82. [PubMed: 10204719]
57. Mohapatra DP, Nau C. Desensitization of capsaicin-activated currents in the vanilloid receptor TRPV1 is decreased by the cyclic AMP-dependent protein kinase pathway. The Journal of biological chemistry. 2003; 278(50):50080–50090. [PubMed: 14506258]
58. Mohapatra DP, Nau C. Regulation of Ca2+-dependent desensitization in the vanilloid receptor TRPV1 by calcineurin and cAMP-dependent protein kinase. The Journal of biological chemistry. 2005; 280(14):13424–13432. [PubMed: 15691846]

59. Mohapatra DP, Wang SY, Wang GK, Nau C. A tyrosine residue in TM6 of the Vanilloid Receptor TRPV1 involved in desensitization and calcium permeability of capsaicin-activated currents. Molecular and cellular neurosciences. 2003; 23(2):314–324. [PubMed: 12812762]

60. Mylius V, Kunz M, Schepelmann K, Lautenbacher S. Sex differences in nociceptive withdrawal reflex and pain perception. Somatosensory & motor research. 2005; 22(3):207–211. [PubMed: 16338828]

61. Nagae M, Hiraga T, Wakabayashi H, Wang L, Iwata K, Yoneda T. Osteoclasts play a part in pain due to the inflammation adjacent to bone. Bone. 2006; 39(5):1107–1115. [PubMed: 16769263]

62. Nersesyan H, Slavin KV. Current aproach to cancer pain management: Availability and implications of different treatment options. Therapeutics and clinical risk management. 2007; 3(3): 381–400. [PubMed: 18488078]

63. Numazaki M, Tominaga T, Toyooka H, Tominaga M. Direct phosphorylation of capsaicin receptor VR1 by protein kinase Cepsilon and identification of two target serine residues. The Journal of biological chemistry. 2002; 277(16):13375–13378. [PubMed: 11884385]

64. Othman AA, Nothaft W, Awni WM, Dutta S. Effects of the TRPV1 antagonist ABT-102 on body temperature in healthy volunteers: pharmacokinetic/ pharmacodynamic analysis of three phase 1 trials. British journal of clinical pharmacology. 2013; 75(4):1029–1040. [PubMed: 22966986]

65. Pan HL, Zhang YQ, Zhao ZQ. Involvement of lysophosphatidic acid in bone cancer pain by potentiation of TRPV1 via PKCepsilon pathway in dorsal root ganglion neurons. Molecular pain. 2010; 6:85. [PubMed: 21118579]

66. Papachristou DJ, Basdra EK, Papavassiliou AG. Bone metastases: molecular mechanisms and novel therapeutic interventions. Medicinal research reviews. 2012; 32(3):611–636. [PubMed: 20818675]

67. Park SI, McCauley LK. Nuclear localization of parathyroid hormone-related peptide confers resistance to anoikis in prostate cancer cells. Endocrine-related cancer. 2012; 19(3):243–254. [PubMed: 22291434]

68. Pharo GH, Zhou L. Pharmacologic management of cancer pain. The Journal of the American Osteopathic Association. 2005; 105(11 Suppl 5):S21–28. [PubMed: 16368904]

69. Pomonis JD, Harrison JE, Mark L, Bristol DR, Valenzano KJ, Walker K. N-(4-Tertiarybutylphenyl)-4-(3-cholorphyridin-2-yl)tetrahydropyrazine -1(2H)-carbox-amide (BCTC), a novel, orally effective vanilloid receptor 1 antagonist with analgesic properties: II. in vivo characterization in rat models of inflammatory and neuropathic pain. The Journal of pharmacology and experimental therapeutics. 2003; 306(1):387–393. [PubMed: 12721336]

70. Rathee PK, Distler C, Obreja O, Neuhuber W, Wang GK, Wang SY, Nau C, Kress M. PKA/AKAP/ VR-1 module: A common link of Gs-mediated signaling to thermal hyperalgesia. The Journal of neuroscience : the official journal of the Society for Neuroscience. 2002; 22(11):4740–4745. [PubMed: 12040081]

71. Ren K, Dubner R. Interactions between the immune and nervous systems in pain. Nature medicine. 2010; 16(11):1267–1276.

72. Rose AA, Siegel PM. Emerging therapeutic targets in breast cancer bone metastasis. Future oncology. 2010; 6(1):55–74. [PubMed: 20021209]

73. Rucci N, Angelucci A. Prostate Cancer and Bone: The Elective Affinities. BioMed research international. 2014; 2014:167035. [PubMed: 24971315]

74. Rucci N, Recchia I, Angelucci A, Alamanou M, Del Fattore A, Fortunati D, Susa M, Fabbro D, Bologna M, Teti A. Inhibition of protein kinase c-Src reduces the incidence of breast cancer metastases and increases survival in mice: implications for therapy. The Journal of pharmacology and experimental therapeutics. 2006; 318(1):161–172. [PubMed: 16627750]

75. Schnizler K, Shutov LP, Van Kanegan MJ, Merrill MA, Nichols B, McKnight GS, Strack S, Hell JW, Usachev YM. Protein kinase A anchoring via AKAP150 is essential for TRPV1 modulation by forskolin and prostaglandin E2 in mouse sensory neurons. The Journal of neuroscience : the official journal of the Society for Neuroscience. 2008; 28(19):4904–4917. [PubMed: 18463244]

76. Schweizerhof M, Stosser S, Kurejova M, Njoo C, Gangadharan V, Agarwal N, Schmelz M, Bali KK, Michalski CW, Brugger S, Dickenson A, Simone DA, Kuner R. Hematopoietic colony-

stimulating factors mediate tumor-nerve interactions and bone cancer pain. Nature medicine. 2009; 15(7):802–807.

77. Shepherd AJ, Mohapatra DP. Tissue preparation and immunostaining of mouse sensory nerve fibers innervating skin and limb bones. Journal of visualized experiments : JoVE. 2012; (59):e3485. [PubMed: 22314687]
78. Shimo T, Kubota S, Yoshioka N, Ibaragi S, Isowa S, Eguchi T, Sasaki A, Takigawa M. Pathogenic role of connective tissue growth factor (CTGF/CCN2) in osteolytic metastasis of breast cancer. Journal of bone and mineral research : the official journal of the American Society for Bone and Mineral Research. 2006; 21(7):1045–1059.
79. Shinoda M, Ogino A, Ozaki N, Urano H, Hironaka K, Yasui M, Sugiura Y. Involvement of TRPV1 in nociceptive behavior in a rat model of cancer pain. The journal of pain : official journal of the American Pain Society. 2008; 9(8):687–699. [PubMed: 18455478]
80. St-Jacques B, Ma W. Prostaglandin E2/EP4 signalling facilitates EP4 receptor externalization in primary sensory neurons in vitro and in vivo. Pain. 2013; 154(2):313–323. [PubMed: 23265688]
81. Stosser S, Schweizerhof M, Kuner R. Hematopoietic colony-stimulating factors: new players in tumor-nerve interactions. J Mol Med (Berl). 2011; 89(4):321–329. [PubMed: 21079906]
82. Takahashi S, Hakuta M, Aiba K, Ito Y, Horikoshi N, Miura M, Hatake K, Ogata E. Elevation of circulating plasma cytokines in cancer patients with high plasma parathyroid hormone-related protein levels. Endocrine-related cancer. 2003; 10(3):403–407. [PubMed: 14503917]
83. Varkaris A, Katsiampoura AD, Araujo JC, Gallick GE, Corn PG. Src signaling pathways in prostate cancer. Cancer metastasis reviews. 2014
84. Wiesenfeld-Hallin Z. Sex differences in pain perception. Gender medicine. 2005; 2(3):137–145. [PubMed: 16290886]
85. Yunoki T, Takimoto K, Kita K, Funahashi Y, Takahashi R, Matsuyoshi H, Naito S, Yoshimura N. Differential contribution of Kv4-containing channels to A-type, voltage-gated potassium currents in somatic and visceral dorsal root ganglion neurons. Journal of neurophysiology. 2014; 112(10): 2492–2504. [PubMed: 25143545]
86. Zhang S, Huang WC, Zhang L, Zhang C, Lowery FJ, Ding Z, Guo H, Wang H, Huang S, Sahin AA, Aldape KD, Steeg PS, Yu D. SRC family kinases as novel therapeutic targets to treat breast cancer brain metastases. Cancer research. 2013; 73(18):5764–5774. [PubMed: 23913825]
87. Zhang X, Huang J, McNaughton PA. NGF rapidly increases membrane expression of TRPV1 heat-gated ion channels. The EMBO journal. 2005; 24(24):4211–4223. [PubMed: 16319926]
88. Zhang XH, Wang Q, Gerald W, Hudis CA, Norton L, Smid M, Foekens JA, Massague J. Latent bone metastasis in breast cancer tied to Src-dependent survival signals. Cancer cell. 2009; 16(1): 67–78. [PubMed: 19573813]
89. Zheng L, Zhu K, Jiao H, Zhao Z, Zhang L, Liu M, Deng W, Chen D, Yao Z, Xiao G. PTHrP expression in human MDA-MB-231 breast cancer cells is critical for tumor growth and survival and osteoblast inhibition. International journal of biological sciences. 2013; 9(8):830–841. [PubMed: 23983616]
90. Zhu W, Oxford GS. Phosphoinositide-3-kinase and mitogen activated protein kinase signaling pathways mediate acute NGF sensitization of TRPV1. Molecular and cellular neurosciences. 2007; 34(4):689–700. [PubMed: 17324588]

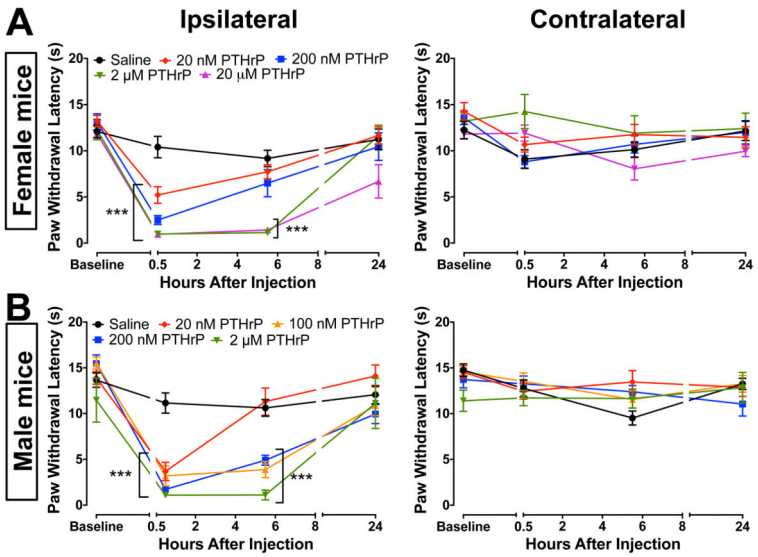

Figure 1.

PTHrP injection into mouse hindpaws leads to the development of thermal hypersensitivity. PTHrP (20 nM, 200 nM, 2 μM and 20 μM; i.pl. injection), as compared to saline injection significantly decreased the PWLs in the ipsilateral paws (left panels) of both female (***A***) and male (***B***) C57BL/6 mice 30 min post-injection, with no significant change in the PWLs of contralateral paws (right panels). Data are presented as mean ± SEM PWLs of mouse hindpaws (n = 8–12 for each group). Male mice (***A***, left panel) presented increased sensitivity in response to PTHrP (20 nM, 100 nM and 200 nM), as compared to females (***B***, left panel). ***$p<0.001$ vs saline-injected (One-way ANOVA with Dunnett's *post hoc* correction).

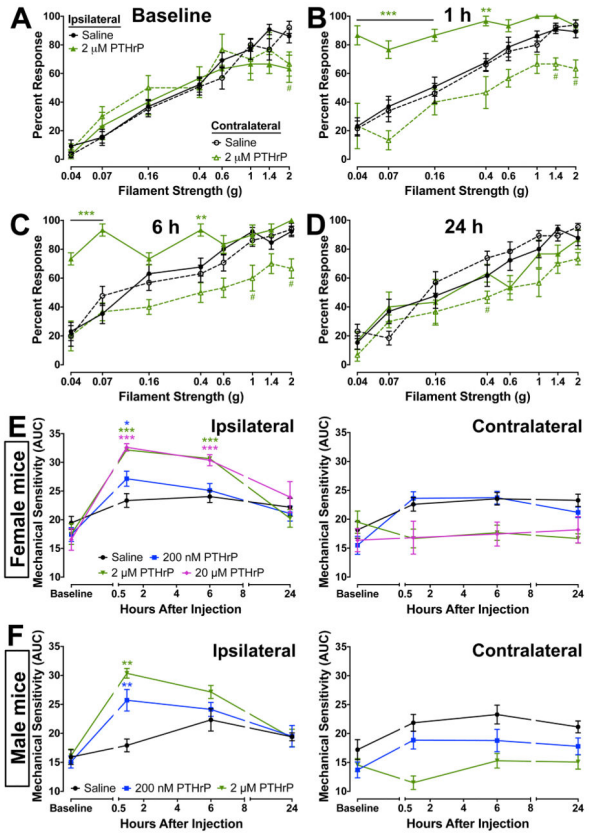

Figure 2.

PTHrP induces mechanical hypersensitivity in mouse hindpaws. ***A–D***, Intraplantar PTHrP injection (2 μM) led to significant enhancement in the extent of mechanical sensitivity in the ipsilateral paws after 1 hour (***B***), as compared to saline injections and baseline measurements (***A***), which was mostly reversed after 6 and 24 hours (***D***). No significant increase was observed in the mechanical sensitivity of contralateral paws (dashed lines; ***A–D***). The area under the curve (AUC) for percent response to Von Frey hair filaments of increasing strength for individual mice (separate ipsilateral and contralateral) at individual time points were calculated and plotted (***E–F***) as mechanical sensitivity at each time points (see methods for details). Data are presented as mean ± SEM calculated mechanical sensitivity (AUC) of mouse hindpaws (n = 6–12 for each group). In both male and female mice PTHrP (200 nM and 2 μM) caused significant mechanical hypersensitivity in ipsilateral paws 1 hour post-injection, which recovered to saline-injected levels by 24 hours (***E***). No significant change in mechanical sensitivity was observed in contralateral paws of female and male mice (dashed lines; ***E–F***). *p<0.05, **p<0.01, and ***p<0.001 vs saline-injected ipsilateral values, and $^{\#}p$<0.05 vs saline-injected contralateral values at respective filament strengths (***A–D***) or time points (***E–F***; One-way ANOVA with Dunnett's *post hoc* correction).

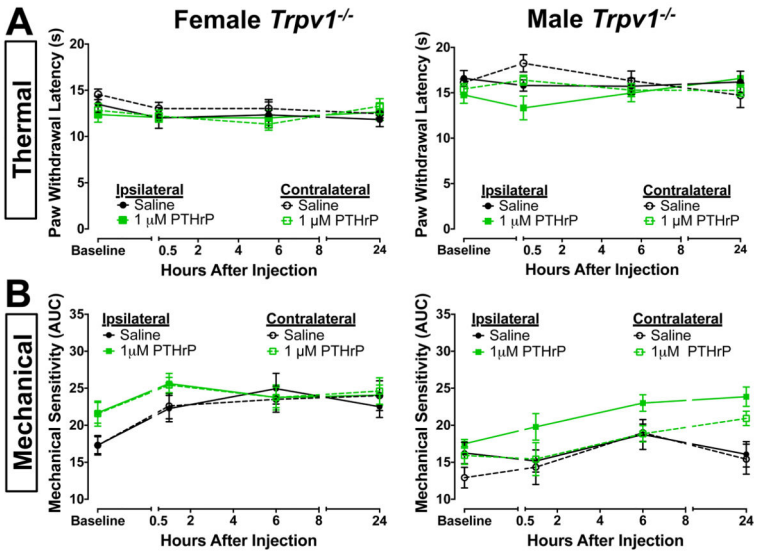

Figure 3.

PTHrP-induced thermal and mechanical hypersensitivity are dependent on TRPV1. Intraplantar PTHrP injection (1 μM), as compared to saline injections, did not lead to any significant change in PWLs (***A***) or the extent of mechanical sensitivity (***B***) in ipsilateral and contralateral hindpaws of both female and male *Trpv1*$^{-/-}$ mice, indicating lack of PTHrP-induced thermal and mechanical hypersensitivity. Data are presented as mean ± SEM PWLs (***A***) and calculated mechanical sensitivity (AUC; ***B***) of mouse hindpaws (n = 6–8 for each group).

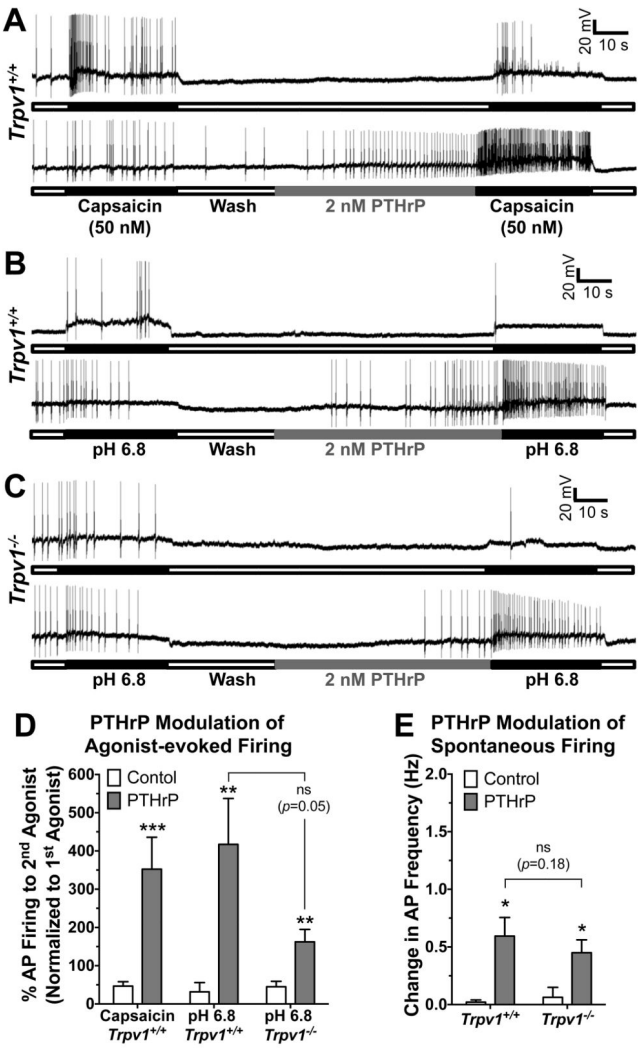

Figure 4.

PTHrP enhances action potential (AP) firing in mouse DRG neurons. Representative traces of capsaicin-evoked (50 nM, 30 sec; ***A***) and extracellular buffer pH 6.8-evoked (***B–C***) AP firings recorded in cultured DRG neurons from *Trpv1*$^{+/+}$ (***A–B***) and *Trpv1*$^{-/-}$ (***C***) mice, without or with PTHrP treatment (2 nM, 1 min) in between two successive agonist applications. PTHrP application itself led to modulation of spontaneous AP firing seen in the lower traces of panels ***A–C***. Quantification of agonist-evoked (capsaicin and pH 6.8) AP firing, before and after PTHrP treatment, from recordings as shown in panels ***A–C***, are shown in panel ***D***. Although there is visible attenuation of pH 6.8-induced AP firing after PTHrP application in DRG neurons from *Trpv1*$^{-/-}$ mice compared to neurons from *Trpv1*$^{+/+}$ mice, this difference is not statistically significant ($p = 0.05$). Panel ***E*** shows the quantification of PTHrP-modulation of spontaneous AP firings resulted upon/during PTHrP application, from recordings as shown in panels ***A–C***, on cultured DRG neurons from *Trpv1*$^{+/+}$ and *Trpv1*$^{-/-}$ mice. The magnitude of PTHrP-modulation of spontaneous AP firings was not significantly different (p=0.18) in neurons from *Trpv1*$^{+/+}$ and *Trpv1*$^{-/-}$ mice. Data in both panels ***D*** and ***E*** are presented as mean ± SEM % change in AP firings or AP

frequency (n = 7–13 neurons in each group). *p<0.05, **p<0.01, and ***p<0.001 vs control (Unpaired Student's T-test).

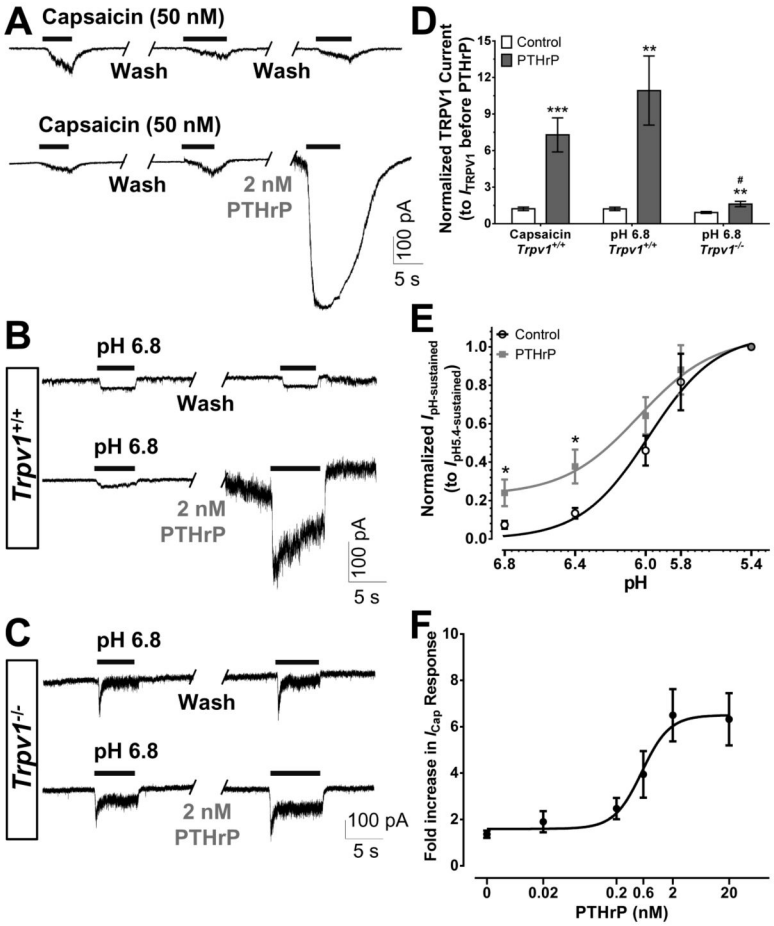

Figure 5.

PTHrP potentiates TRPV1 channel activity in mouse DRG neurons. Representative traces of two successive capsaicin-activated (I_{Cap}; ***A***) and extracellular buffer pH 6.8-activated ($I_{pH\ 6.8}$; ***B–C***) currents, with or without PTHrP treatment (2 nM, 1 min) in between, in cultured DRG neurons from *Trpv1*$^{+/+}$ (***A–B***) and *Trpv1*$^{-/-}$ (***C***) mice. ***D***, Quantification of the ratio of 3rd vs 2nd peak I_{Cap} or 2nd vs 1st peak $I_{pH\ 6.8}$ under control and PTHrP-treatment conditions in cultured DRG neurons from *Trpv1*$^{+/+}$ and *Trpv1*$^{-/-}$ mice. ***E***, pH dose-response curve for the sustained component of proton-induced inward currents, normalized to $I_{pH\ 5.4}$ from cultured mouse DRG neurons, with or without PTHrP treatment (2 nM, 1 min). PTHrP significantly increased the magnitude of $I_{pH\text{-}sustained}$ at pH 6.8 and 6.4, without any significant change in the EC_{50} of the dose response relationship. ***F***, PTHrP dose-response curve determined from the effect of increasing concentrations of PTHrP (20 pM, 200 pM, 600 pM, 2 nM, and 20 nM) on fold-increase in peak I_{Cap} magnitude in cultured mouse DRG neurons. EC_{50} = 0.56 nM (95% confidence interval −0.25 nM to 1.26 nM). Data in panels ***D–F*** are presented as mean ± SEM and fitted value ± SE of fit (n = 10–17 neurons in each group). *p<0.05, ***p<0.01, and ***p<0.001 vs control of respective genotypes, and $^{\#}p$<0.05 vs PTHrP group for $I_{pH\ 6.8}$ in panel ***D*** (Unpaired Student's T-test).

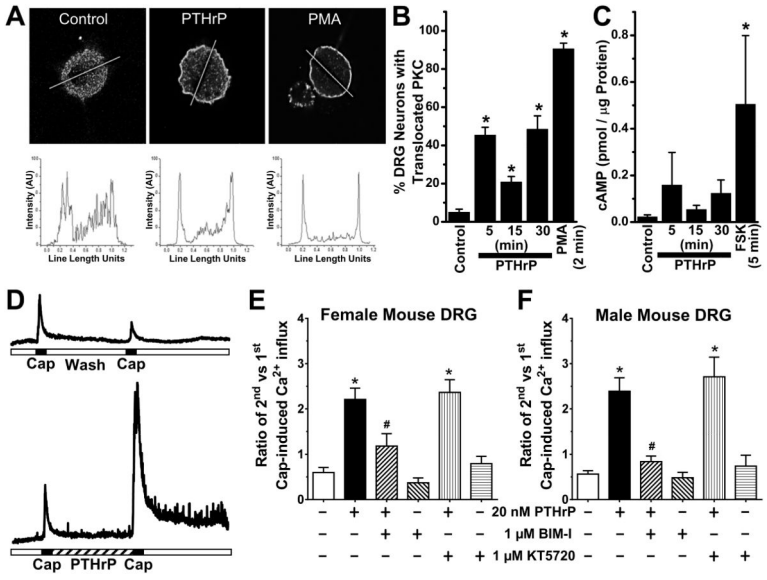

Figure 6.

PTHrP exposure of mouse sensory neurons leads to PKC activation, and is critical for potentiation of TRPV1 activity. ***A***, Representative confocal microscopic images (top row) of cultured mouse DRG neurons, with or without the treatment of PTHrP (10 nM, 2 min) or PMA (100 nM, 2 min), immunostained with anti-PKCε antibody. Traces in the bottom row depict PKCε distribution profiles across the respective drawn line determined using NIH Image J. ***B***, Quantification of percentage of cultured mouse DRG neurons with PKCε translocation (n = >100 cells in each group obtained from ≥3 batches of cultures). ***C,*** cAMP ELISA experiments showed no significant increase in cAMP levels in mouse DRG neurons treated with PTHrP (10 nM). Forskolin (10 μM, 5 min) significantly increased cellular cAMP levels compared to untreated control DRG neurons. ***D***, Representative traces of Ca^{2+} influx in cultured mouse DRG neurons, in response to two successive capsaicin applications (50 nM, 15 sec), with or without PTHrP treatment (20 nM, 5 min) in between. ***E–F***, Quantification of the ratio of 2^{nd} vs 1^{st} capsaicin-induced Ca^{2+} influx, under control and 20 nM PTHrP treatment conditions. Neurons were treated with inhibitors of PKC (BIM-I; 1 μM), PKA (KT5720; 1 μM) and Src (PP2; 100 nM) before the 1^{st} capsaicin application and continued throughout PTHrP or control buffer applications. Inhibition of PKC, but not Src or PKA attenuated PTHrP-sensitization of capsaicin-induced Ca^{2+} influx in cultured DRG neurons from both female (***E***) and male (***F***) mice. Data are presented as mean ± SEM (n = 11–52 neurons in each group). *p<0.05 vs untreated control (One way ANOVA with Dunnett's *post hoc* correction), and $^{\#}p$<0.05 vs PTHrP group in panels ***E–F*** **(**Unpaired Student's T-test).

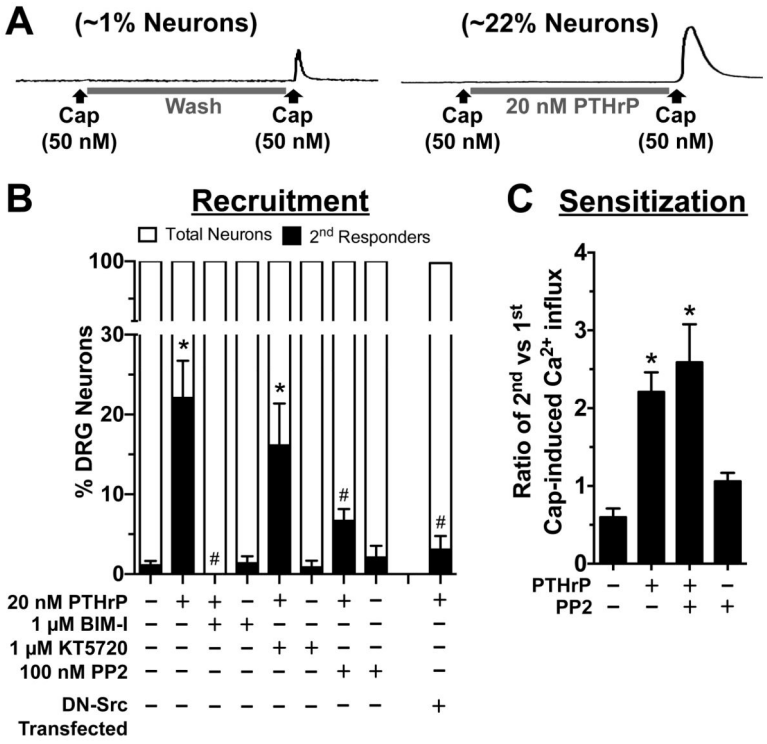

Figure 7.

PTHrP enhances the proportion of TRPV1-responsive mouse sensory neurons that is dependent on the activity of PKC and Src. ***A***, Representative traces showing Ca^{2+} influx in cultured mouse DRG neurons, in response to 2nd, but not 1st capsaicin application (50 nM, 15 s), only after PTHrP exposure (20 nM, 5 min). ~1% of control DRG neurons show Ca^{2+} responses to only 2nd capsaicin application, whereas PTHrP exposure leads to 2nd capsaicin-induced Ca^{2+} influx in ~22% DRG neurons (n= >10 experimental batch). ***B***, PTHrP increased the number of neurons responding to 2nd capsaicin application, quantified as percent 2nd capsaicin responders per experiment. Inhibition of PKC (with BIM-I) and Src (with PP2), but not PKA (with KT5720) significantly reduced the number of 2nd capsaicin responders. PTHrP application led to no significant increase in the number of 2nd capsaicin responders in cultured mouse DRG neurons transfected with dominant-negative Src (DN-Src), as shown in panel ***B*** last bar data set. ***C,*** Quantification of the ratio of 2nd vs 1st capsaicin-induced Ca^{2+} influx, under control and PTHrP (20 nM, 5 min) treatment conditions, similar to the experiments in figure 6 panels D–E, with or without the co-application of PP2 (100 nM) before the 1st capsaicin application and continued throughout PTHrP or control buffer applications. Inhibition of Src did not attenuate PTHrP-induced sensitization of capsaicin-induced Ca^{2+} influx in cultured mouse DRG. Data are presented as mean ± SEM for panels ***B*** (n = 7–16 experiments in each group) and ***C*** (n = 49–56 neurons in each group). *$p<0.05$ vs untreated control, and $^{\#}p<0.05$ vs PTHrP group (One way ANOVA with Dunnett's *post hoc* correction).

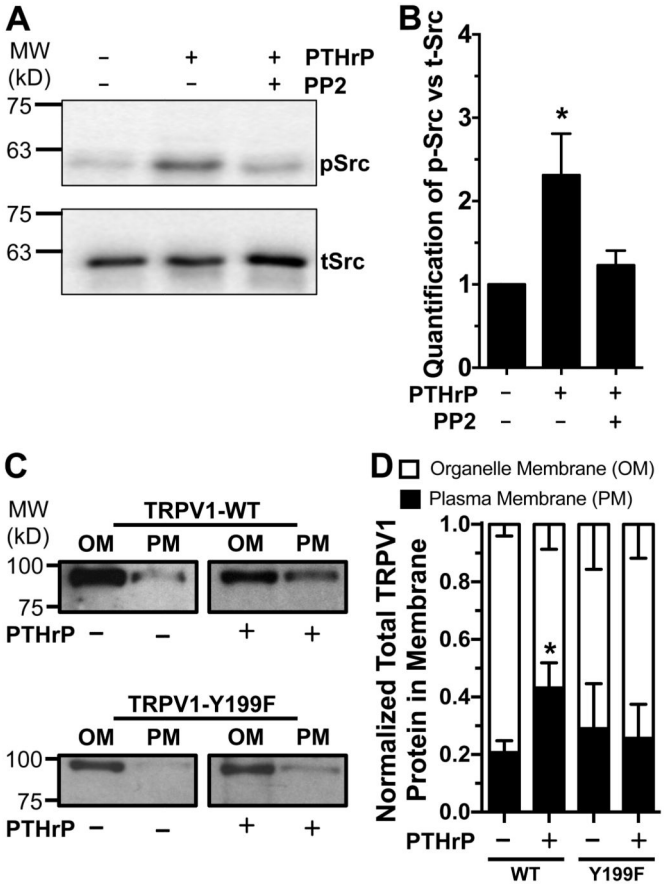

Figure 8.

PTHrP enhances Src phosphorylation in DRG neurons and increases the TRPV1 protein level in plasma membrane. ***A,*** Representative immunoblot, from four independent experiments, showing PTHrP exposure (20 nM, 10 min) leads to Src activation in cultured mouse DRG neurons, as quantified by enhanced phospho-Src (pSrc) levels normalized to total-Src (tSrc) levels shown in panel ***B***. This effect was reduced by co-application of Src inhibitor PP2 with PTHrP. ***C,*** Representative immunoblot showing PTHrP exposure (20 nM, 10 min) leads to an increase in TRPV1 protein levels in the plasma membrane (PM) vs intracellular organelle membrane (OM) in lysates of HEK293T cells co-transfected with rTRPV1-WT-myc and rPTH1R-YFP. This effect was absent in the lysates of HEK293T cells co-transfected with the Src phosphorylation site mutant rTRPV1-Y199F-myc and rPTH1R-YFP. Results from multiple experiments were quantified and presented as fraction of plasma membrane TRPV1 protein levels out of normalized total membrane TRPV1 (***D***). Numbers on the left in panels ***A*** and ***C*** indicate relative mobility of protein molecular weight markers (in kilodalton; kD). Data are presented as mean ± SEM (n = 4 for panel ***B***, and n = 3–6 transfection batches for panel ***D***). *p<0.05 vs untreated control (One way ANOVA with Dunnett's *post hoc* correction, and unpaired Student's T-test).

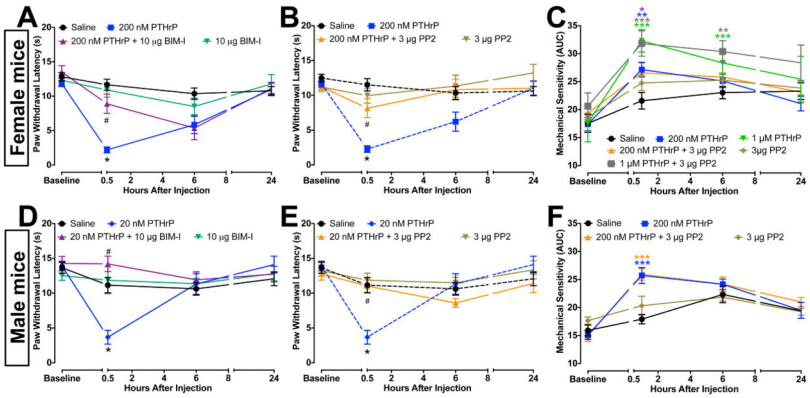

Figure 9.

PTHrP-induced thermal, but not mechanical hypersensitivity in mouse hind paws were attenuated by inhibition of PKC and Src. ***A, B, D*** and ***E,*** Thermal hypersensitivity elicited by PTHrP injection (200 nM, i.pl.) in the ipsilateral hindpaws of mice was attenuated by co-injection of inhibitors of PKC (10 µg BIM-I; ***A*** and ***D***) and Src (3 µg PP2; ***B*** and ***E***) in both female (***A–B***) and male (***D–E***) mice. Injection (i.pl.) of BIM-I (10 µg) or PP2 (3 µg) alone did not lead to any significant change in the PWLs, as compared to saline-injected controls (***A, B, D,*** and ***E***). Co-injection of PP2 (3 µg) did not attenuate the mechanical hypersensitivity elicited by 1 µM and 200 nM PTHrP in female (***C***) and male (***F***) mice. No change in thermal or mechanical sensitivity was observed in either sex of mice in the contralateral paws (not shown). Dotted lines in panels ***B*** and ***E*** indicate the same data sets presented in panels ***A*** and ***D***, respectively. Injection (i.pl.) of PP2 (3 µg) alone did not lead to any significant change in calculated mechanical sensitivity, as compared to saline-injected controls (***C, F***). Data are presented as mean ± SEM PWLs, and as mean ± SEM of calculated mechanical sensitivity (AUC) of mouse hindpaws (n = 6–12 for each group). *$p<0.05$, **$p<0.01$, and ***$p<0.001$ vs saline-injected respective control groups, and $^{\#}p<0.05$ vs respective PTHrP groups (One-way Anova with Dunnett's *post hoc* correction).